Journal of Geochemical Exploration 255 (2023) 107324

Contents lists available at ScienceDirect

Journal of Geochemical Exploration

journal homepage: www.elsevier.com/locate/gexplo

Background and geochemical baseline values of chalcophile and siderophile elements in soils around the former mining area of Abbadia San Salvatore (Mt. Amiata, southern Tuscany, Italy)

Federica Meloni [a,b,*], Barbara Nisi [b], Caterina Gozzi [a,c], Valentina Rimondi [a], Jacopo Cabassi [b], Giordano Montegrossi [b], Daniele Rappuoli [d,e], Orlando Vaselli [a,b]

[a] Department of Earth Sciences, Via G. La Pira, 4, 50121 Firenze, Italy
[b] CNR-IGG Institute of Geosciences and Earth Resources, Via G. La Pira, 4, 50121 Firenze, Italy
[c] NBFC, National Biodiversity Future Center, Palermo 90133, Italy
[d] Unione dei Comuni Amiata Val d'Orcia, Unità di Bonifica, Via Grossetana 209, 53025 Piancastagnaio, Siena, Italy
[e] Parco Museo Minerario di Abbadia San Salvatore - Via Suor Gemma, 53021, Abbadia San Salvatore 1, Siena, Italy

ARTICLE INFO

Keywords:
Mt. Amiata
Mercury mines
Background values
Geochemical baseline
Potentially toxic elements

ABSTRACT

Background and geochemical baseline values of Potentially Toxic Elements (PTEs) in soils developed on natural or anthropogenically-affected areas are increasingly important parameters as they represent highly useful tools at local, regional, national and European level. While background values are mostly applied to uncontaminated areas to verify the presence of high to anomalous concentrations of PTEs due to geogenic sources, the geochemical baseline values are better representing those areas where the anthropogenic activities have altered more or less significantly the background values. This is the case of the Municipality of Abbadia San Salvatore, mostly lying above the volcanic products of Mt. Amiata (Tuscany, central Italy) and, subordinately, above sedimentary formations, where >100 years of exploitation of cinnabar (HgS) and production of liquid mercury have affected the environmental matrices, including the pedosphere compartment. Consequently, 51 top-soils and 51 sub-soils, developed on the volcanic and sedimentary domains were collected and analyzed for PTEs (Hg, As, Sb, Cr, Co, Ni, Cu and V). A CoDA (Compositional Data Analysis) approach (robust Principal Component Analysis) combined with geochemical mapping allowed to account for the compositional nature of geochemical data and define the spatial distribution of the investigated chalcophile and siderophile elements. The results obtained by CoDa are useful to understand data variability and relative variations of the elements compared to the barycenter of the total composition. Independently by the substratum (volcanic or sedimentary), the concentrations of Hg, As, Sb, Cr, Co, Ni, Cu and V were highly variable and up to 258, 276, 110, 261, 32, 132, 80 and 173 mg/kg, respectively. Owing to the significant differences between the two geological domains, the two datasets were considered separately in order to define the geochemical baseline values of the analyzed PTEs computed using ProUCL 5.2.0 software. Accordingly, the geochemical baseline values of Hg, As, Cr, Co and V were much higher than the values imposed by the Italian Legislative Decree 152/06, suggesting the importance of exploring the geological features of the investigated territories and their anthropic history, particularly in Italy where poly-metallic sulfide ore deposits have been exploited in many regions since the Etruscan and Roman times.

1. Introduction

Potentially Toxic Elements (PTEs) (Pourret and Hursthouse, 2019) can be regarded as stable and enduring environmental contaminants and soil is the most prone exogeneous matrix able to accumulate them (Qingjie and Jun, 2008; Marchand et al., 2011; Mazurek et al., 2017). The presence of PTEs in the pedological cover depends on many factors such as the mineralogical composition of the bedrock (Cabral Pinto et al., 2017) and soil formation processes, the latter being able to govern the distribution of trace elements along the soil profile (e.g. Kabata-

* Corresponding author at: Department of Earth Sciences, Via G. La Pira, 4, 50121 Firenze, Italy.
E-mail address: federica.meloni@unifi.it (F. Meloni).

https://doi.org/10.1016/j.gexplo.2023.107324
Received 12 June 2023; Received in revised form 28 September 2023; Accepted 1 October 2023
Available online 14 October 2023

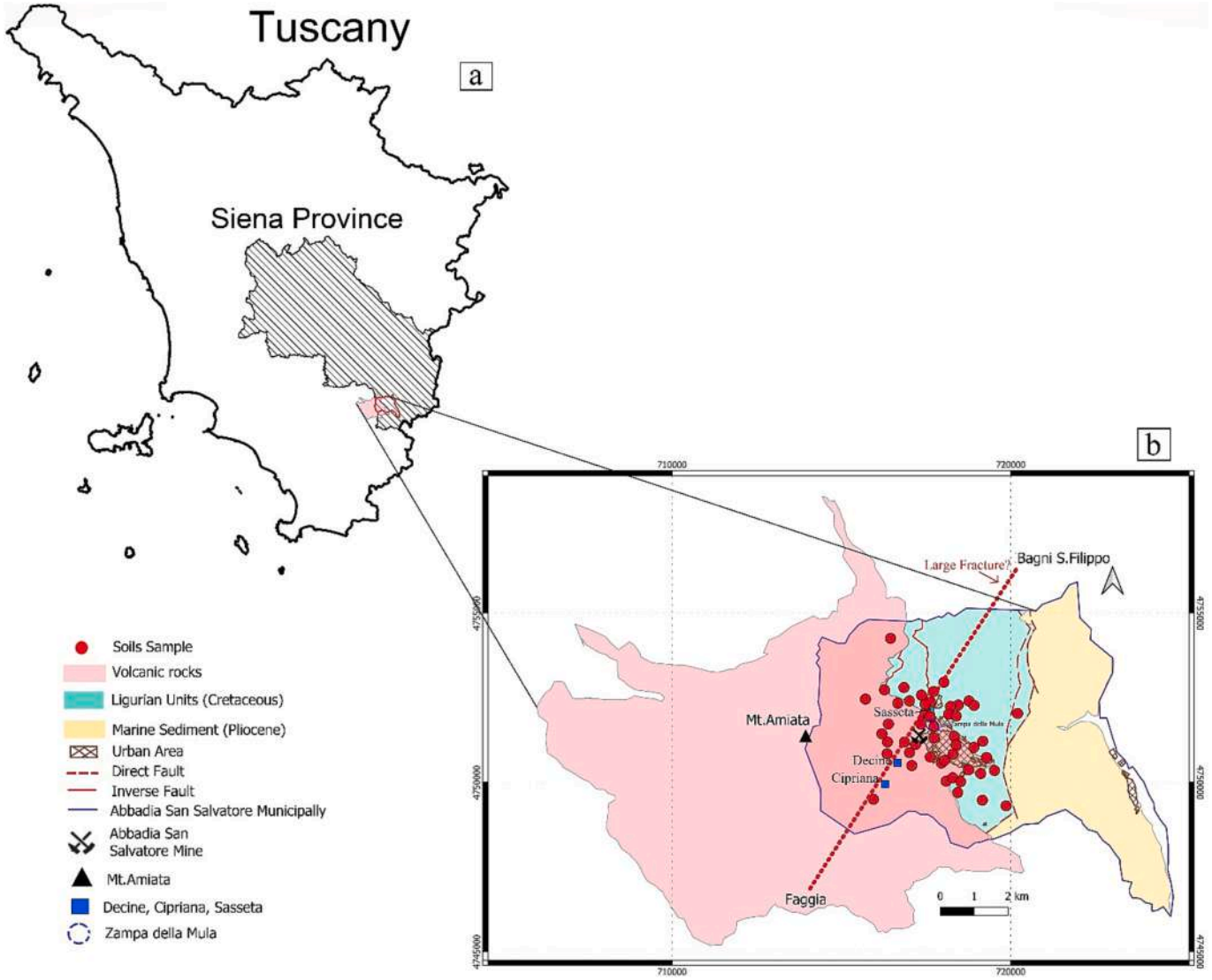

Fig. 1. a, b: Simplified geological map of the study area (modified after Marroni et al., 2015). The red circles indicate the soil sampling sites. According to Conticelli et al. (2015), the volcanic rocks (0.3–0.2 Ma) are mostly consisting of a trachydacitic basal complex, exogeneous lava domes (Pianello Fm, e.g. Principe et al., 2018; Vezzoli and Principe, 2023) and an olivine-latite lava flow. The External and Internal Ligurian Units include the Santa Fiora Fm and the Argille a Palombini Fm. The dashed line is the trace of a likely NE-SW-oriented Large Fracture as suggested by Forconi (2011) (see text for details).

Pendias, 2010). In most cases, PTEs occur in the soil at trace levels (<1000 mg/kg) and their concentration is rarely toxic during the physicochemical alteration of the parent material. Nevertheless, exposure to PTEs can have adverse health effects (e.g. Giaccio et al., 2012 and reference therein) and increases the probability of cancer development in humans when they are exposed to naturally and/or anthropogenically-enriched substrata (Tarvainen and Kallio, 2002; Cicchella et al., 2005; Frattini et al., 2006; Albanese et al., 2007; Galan et al., 2008; Cicchella et al., 2022) such as those occurring in urban/suburban areas and active or abandoned mining sites (e.g. Nriagu and Pacyna, 1988; Karn et al., 2021). As a consequence, it is of pivotal importance to understand their content and geochemical behavior in soils to define the thresholds at which they can be considered not harmful for human beings and, generally speaking, ecosystems. Moreover, establishing the source (natural or anthropic) of PTEs is an additional and critical parameter to undertake during remediation operations in decommissioned mining areas.

According to the Italian Legislative Decree 152/2006, the threshold values recommended for soils do not necessarily reflect the chemical and mineralogical conditions and the geological formations onto they are developed. This implies that the threshold values can be modified at local or site-specific level in agreement with the Agency of Environmental Protection (ARPA) and regional authorities (Cicchella et al., 2022).

The term "geochemical baseline", presented in 1933 at the International Geological Correlation Program as the Global Geochemical Baselines (Salminen and Tarvainen, 1997; Salminen and Gregorauskiene, 2000; Galan et al., 2008), concerns the natural concentration variability of an element in superficial environments at a determined place and time (Santos-Francés et al., 2017). Similarly, Salminen and Gregorauskiene (2000), Frattini et al. (2006), Albanese et al. (2007) and Galan et al. (2008) defined the term geochemical baseline as the actual content of an element in environmental matrices at a given point in time. It includes the geogenic concentration (or "natural background", i.e. the environmental conditions prior of any anthropogenic activity; e.g. Nordstrom, 2015; Pasquetti et al., 2020) and the anthropogenic contribution (Tarvainen and Kallio, 2002; Cicchella et al., 2005; Frattini et al., 2006; Albanese et al., 2007; Galan et al., 2008; Cicchella et al., 2022). It has been demonstrated that the natural background can vary from one area to another within the same region (Cicchella et al., 2022).

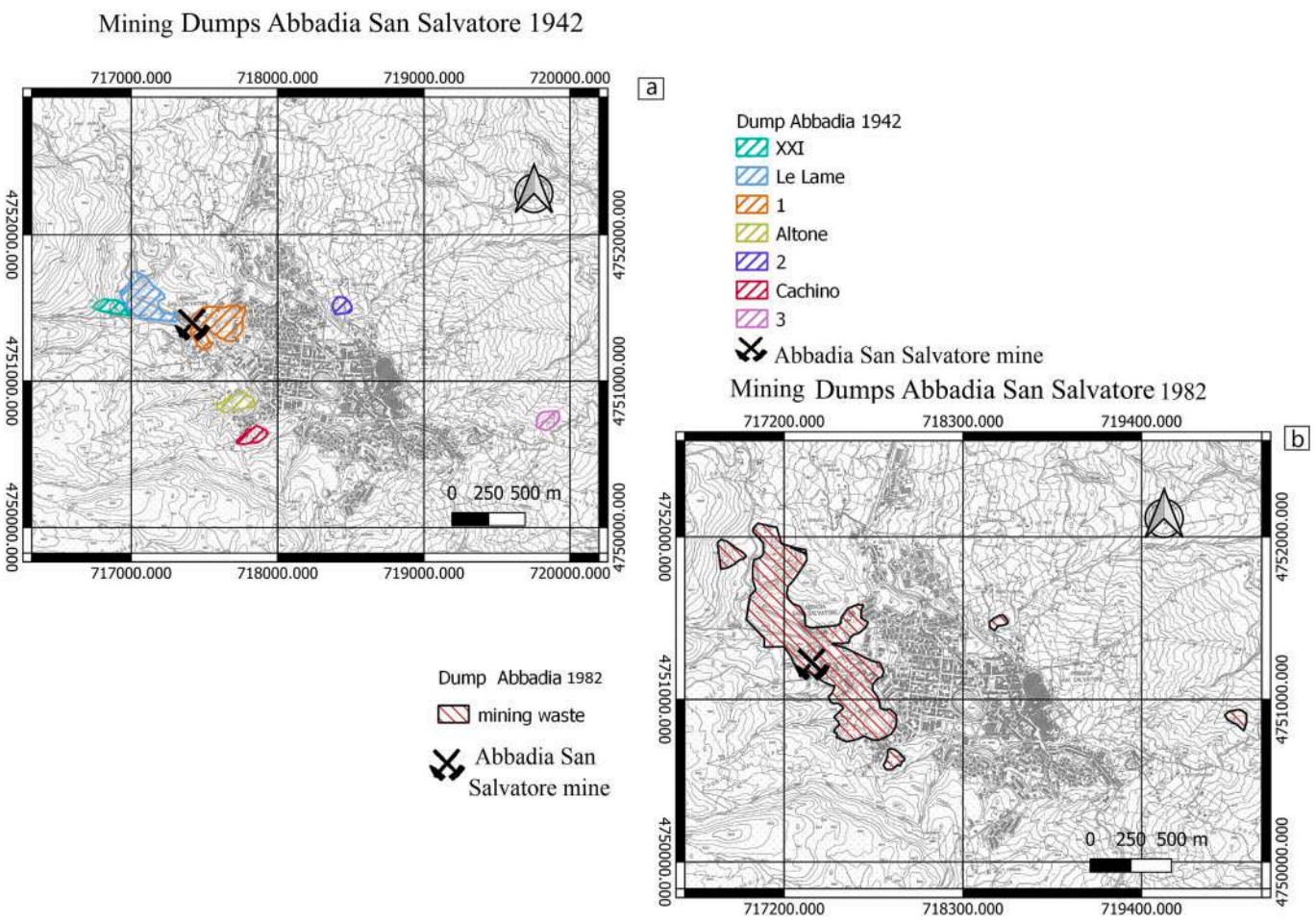

Fig. 2. The 1942 (a) and 1982 (b) Abbadia San Salvatore mining dumps. 1, 2 and 3 refer to nameless mining dumps.

Consequently, it is extremely difficult to establish a natural background level and a single background concentration in a specific area. For this reason, the geochemical baseline, being expressed as concentration (or concentration interval), is a more useful parameter since it represents the conditions in a certain area where the human activity has already impacted the environment due to industry, mining and/or agriculture practices (Facchinelli et al., 2001; Santos-Francés et al., 2017).

The definition of geochemical baseline can suitably be applied to soils from abandoned or active mining areas and surroundings, such as that of Abbadia San Salvatore (southern Tuscany, Italy), where cinnabar (HgS)-ore deposits have been exploited for almost a century. In such areas, the aim is to assess the current quality state of the environment and provides guidelines and quality standards to support the environmental legislation and policy-making actors (Santos-Francés et al., 2017). In agreement with Tanelli (1983), Klemm and Neumann (1984), Dini (2003) and Brogi et al. (2011), Hg mineralization in this area was due to shallow hydrothermal convective systems related to geothermal anomalies that, in turn, were associated with the emplacement of granitoid rocks at mid- and upper-crustal levels in southern Tuscany during the Plio-Pleistocene. The emplacement of hydrothermal breccia bodies and the ascent of hydrothermal fluids also allowed the formation of Hg-rich deposits within argillitic and calcareous strata (Protano and Nannoni, 2018). The circulating hydrothermal fluids favored the precipitation of cinnabar, as well as that of Sb- and As-sulfides.

In this study, a CoDa (Compositional Data Analysis) approach (robust Principal Component Analysis) in combination with geochemical mapping was adopted to: i) define the spatial distribution of chalcophile (As, Cu, Hg and Sb) and siderophile (Co, Cr, Ni and V) elements in the top- and sub-soils of the Municipality of Abbadia San Salvatore and ii) identify sources and pathways of these elements linked to bedrock and soil formation processes and anthropogenic inputs. As suggested by several investigations (e.g. Filzmoser et al., 2009; Reimann et al., 2012; Buccianti et al., 2018; Ghezelbash et al., 2020), multivariate statistical analysis has demonstrated to provide a good reliability in characterizing complex geochemical systems. However, geochemical data are compositional data and only give relative information because they are not free to vary independently, as they pertain to a constrained sample space with a D-1 dimension (D number of variables), named *simplex* (Aitchison, 1986). Therefore, appropriate data transformations (e.g. isometric log-ratio or centered log-ratio transformations) need to be applied to transform the data in real coordinates in a way that classical statistical methods can be applied. Additionally, the Geochemical Baselines (GB) of chalcophile (As, Cu, Hg and Sb) and siderophile (Co, Cr, Ni, and V) elements were then computed using ProUCL 5.2.0 software developed by USEPA (2022), following a consolidated classical approach so that comparisons with national and international benchmark could be performed (e.g. Turkey, 1977; Gilbert, 1987)

2. Study area and brief outlines on the past mining activity

The study area covers approximately 25.6 km^2 and is part of the Municipality of Abbadia San Salvatore. It includes the homonymous town (ca. 6000 inhabitants), and is located in the eastern sector of the silicic volcanic complex of Mt. Amiata (southern Tuscany; Ferrari et al., 1996) (Fig. 1). The volcanic products of Mt. Amiata (0.3–0.2 Ma) are mainly trachydacites and, to a lesser extent, rhyodacites and olivine-latites (Ferrari et al., 1996; Conticelli et al., 2015; Laurenzi et al., 2015) and are the expression of the most recent volcanic events in

Table 1
Geographic coordinates, pH, and concentrations (mg/kg) of Hg, As, Sb, Cr, Cu, Co, V, and Ni in the seven rocks representative of the outcropping geological formations in the study area. The arithmetic mean concentration (mg/kg) of PTEs from the literature is also reported for comparison. References: a) Gao et al. (1998); b) Geochemical Earth Reference Model (GERM, Staudigel et al., 1996) Reservoir Database; c) Salminen et al. (2005); d) Reimann and de Caritat (1998); e) Condie (1993); f) Kemp and Hawkesworth (2004).

Name	X	Y	pH	Hg	As	Sb	Cr	Cu	Co	V	Ni
	WGS84-32N	WGS84-32N		mg/kg	mg/kg	mg/kg	mg/kg	mg/kg	mg/kg	mg/kg	mg/kg
APA	717,466	4,753,335	8.41	0.008	1.0	4.0	69.8	67.8	7.7	85.0	55.0
SFR1	719,434	4,751,361	9.00	0.015	1.0	1.0	33.6	23.0	4.7	31.8	24.2
SFR 2	717,887	4,753,501	8.72	<0.015	1.0	<1.0	75.2	3.7	2.5	8.7	45.8
SFR 3	719,425	4,751,852	8.42	<0.015	1.0	3.0	74.2	37.6	6.9	53.8	89.8
VULC	716,197	4,752,877	4.69	0.0105	13.0	<1.0	94.5	49.3	14.6	62.6	64.9
OLF1	716,205	4,751,428	6.10	0.0403	8.0	<1.0	39.5	49.0	18.4	82.5	42.8
QRT	716,864	4,751,567	6.09	0.68	6.0	<1.0	4.5	10.1	5.3	12.9	2.4
Clay				0.18[d]	10.6–22.5[b]	0.98–1.5[a]	90–507[e]	45[d]	18-31[e]	100-138[a]	70[d]
Limestone				0.05–0.2[a]	0.7–4.7[b]	0.09–0.4[a]	8–13[a]	6[d]	2.1–3.0[a]	4–20[a]	5[c]
Sialic rocks				0.03[d]	4.5[b]	0.12–0.13[a]	8–35[e]	6.6–19[f]	6–12[e]	23–45[f]	1–15[f]
Mean sialic rock in this study				0.24	9.0	<1.0	41.2	36.1	12.7	52.6	36.7
Mean limestone in this study				0.009	1.0	1.5	61.0	24.4	4.7	31.4	53.3

Table 2
Minimum, Maximum, Arithmetic Mean, Median, Standard Deviation (SD), and Skewness of pH, Hg, As, Sb, Cr, Cu, Co, V, and Ni in the 51 top-soils from the Municipality of Abbadia San Salvatore and in Europe median top-soils (Salminen et al., 2005). All concentrations, except pH, are in mg/kg.

	Minimum	Maximum	Mean	Median	SD	Skewness	Median top-soils Europe
pH	4.64	7.43	5.90	6.01	0.85	0.03	5.51
Hg	0.16	211	10.89	1.97	34.60	4.69	0.04
As	<1	63.3	18.6	14.8	16.7	1.0	6.0
Sb	<1	12.0	2.3	1.0	2.5	1.8	0.6
Cr	11.8	157.5	62.2	52.8	37.4	0.7	22.0
Cu	6.1	51.8	23.6	16.6	14.5	0.6	12.0
Co	1.8	22.1	11.2	10.5	4.7	0.3	8.0
V	13.6	148.9	65.3	57.1	32.4	0.5	33.0
Ni	<1	104.5	31.7	27.8	24.6	1.0	14.0

Table 3
Minimum, Maximum, Arithmetic Mean, Median, Standard Deviation (SD), and Skewness of pH, Hg, As, Sb, Cr, Cu, Co, V, and Ni in the 51 sub-soils from the Municipality of Abbadia San Salvatore and in Europe median sub-soils (Salminen et al., 2005). All concentrations, except pH, are in mg/kg.

	Minimum	Maximum	Mean	Median	SD	Skewness	Median Sub-soils Europe
pH	4.75	7.31	6.16	6.39	0.71	−0.41	5.79
Hg	0.03	268.00	13.13	1.25	49.90	4.53	0.02
As	<1	276.2	25.9	16.9	40.8	4.6	5.0
Sb	<1	109.6	4.3	0.9	15.2	6.5	0.4
Cr	8.3	261.6	76.8	66.0	52.9	1.2	24.0
Cu	2.0	80.1	25.5	20.4	15.4	1.0	13.0
Co	2.7	31.7	12.1	11.8	5.7	1.0	7.0
V	13.8	172.6	69.0	59.7	33.6	0.6	33.0
Ni	<1	132.3	28.6	36.7	29.8	1.3	18.0

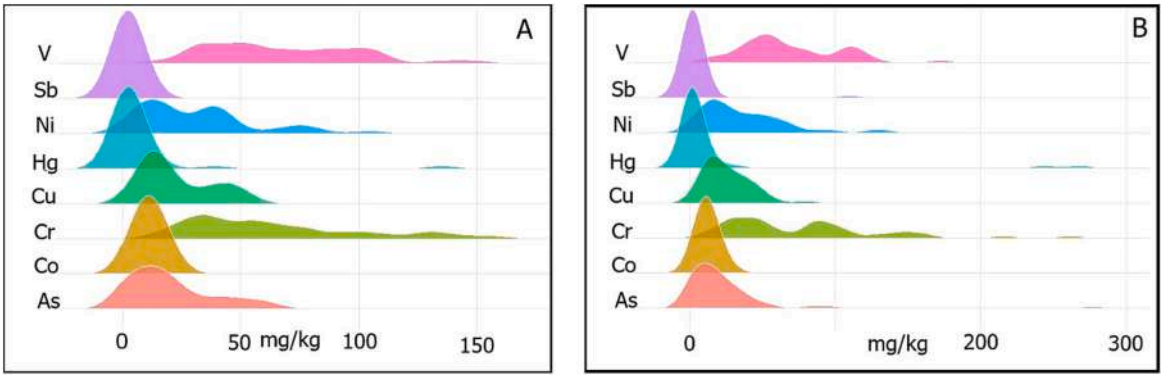

Fig. 3. Ridge-plots of A) top-soils and B) sub-soils representing the Kernel density of the investigated elements.

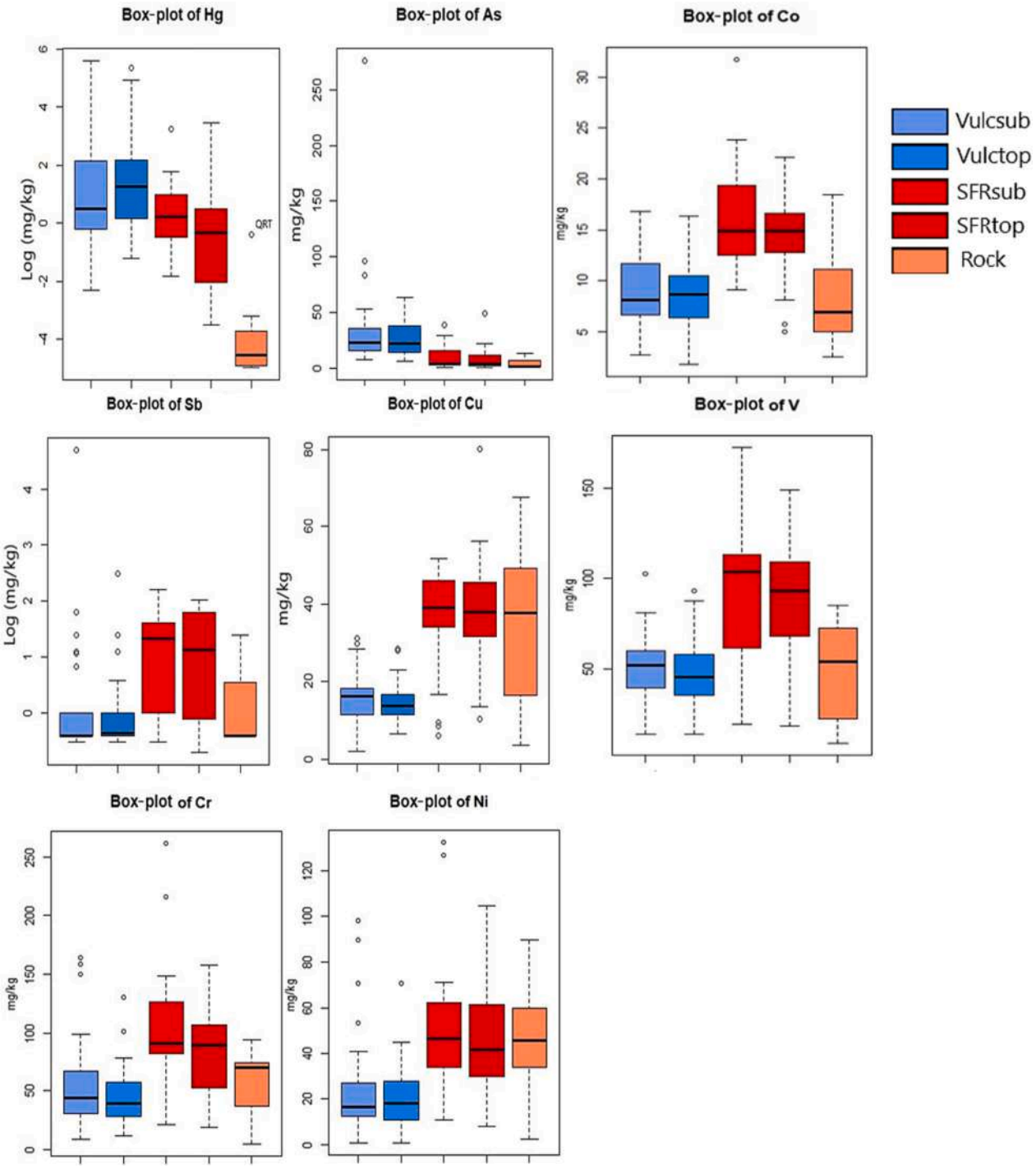

Fig. 4. Box-plots of the analyzed PTSs divided according to the different lithologies. The Hg and Sb concentrations are reported in log-scale to better evidence the differences in terms of lithological variability. The volcsub, volctop, SFRsub, SFRtop, and rock represent the volcanic sub-soils, volcanic top-soils, limestone-siliciclastic sub-soils, limestone-siliciclastic top-soils, and rocks, respectively.

Tuscany (Vezzoli and Principe, 2023). The volcanic deposits lie over a substrate consisting of Cretaceous turbidites, e.g. calcareous and siliciclastic turbidities (Marroni et al., 2015), belonging to the External and Internal Ligurian Domain (e.g. Santa Fiora *Formation* (*Fm*) and Argille a Palombini *Fm*) and Pliocene marine sediments deposited in the Radicofani basin (Ferrari et al., 1996; Liotta, 1996; Pandeli et al., 2005; Brogi et al., 2011; Marroni et al., 2015; Pandeli et al., 2017).

The Mt. Amiata area is an important site for the exploitation of geothermal fluids. The Mt. Amiata and Larderello-Travale-Radicondoli geothermal fields are the only areas in Italy where electric energy is produced from endogenous fluids (e.g. Gianelli et al., 1988; Bellani et al., 2004). In the past, the eastern-southern portion of Mt. Amiata was also an important district for the production of liquid Hg from cinnabar. There are indeed several Hg-rich ore deposits which extend along a NE-SW belt (Brogi et al., 2011) and the most important site to process HgS was located at Abbadia San Salvatore mine (ASSM). It has been estimated that about 50 % of the total Hg production from the Mt. Amiata district was derived by this mining area (e.g. Cipriani and Tanelli, 1983; Vaselli et al., 2013; Rimondi et al., 2015; Pribil et al., 2020). Cinnabar was the primary ore mineral and was often associated with other Fe-

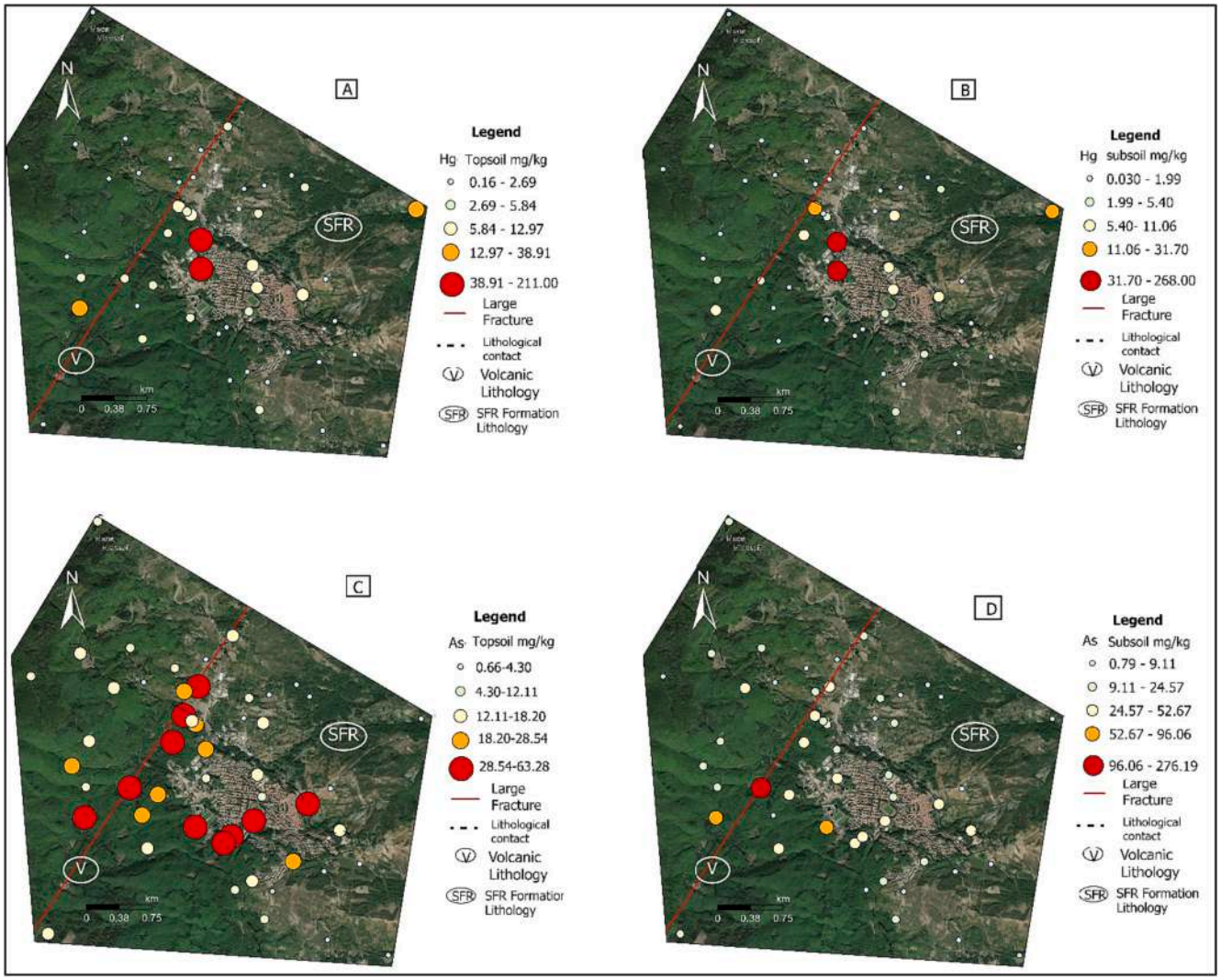

Fig. 5. Hg top-soil (A) and sub-soil (B) dot-maps; As top-soil (C) and sub-soil (D) dot-maps. Maxar, Microsoft indicates a high-resolution satellite and aerial imagery available on ArcGis-Pro 3.0. The dashed black curve represents the lithological contact between the volcanic and sedimentary domains, while the red line represents the Large fracture (Forconi, 2011). The concentration intervals are from the Fisher-Jenks classification. (For interpretation of the references to color in this figure legend, the reader is referred to the web version of this article.)

sulfides (e.g. pyrite and marcasite) and realgar and orpiment, while stibnite was rarely encountered (Morteani et al., 2011; Rimondi et al., 2014; Chiarantini et al., 2016; Pribil et al., 2020).

Significantly, the processing plant, which mostly distributes along the road heading to the summit of Mt. Amiata, is intimately connected to the urban center of Abbadia San Salvatore. The mining processes have had an important environmental impact since all matrices (soil, water and air) were affected by Hg (e.g. Bargagli et al., 1987; Barghigani and Ristori, 1994, 1995; Ferrara et al., 1998; Rimondi et al., 2012, 2014, 2015; Vaselli et al., 2017, 2019).

The mercury mine operated underground (down to 470 m below ground level), covering 35 km of galleries. The Hg content at ASSM was relatively low (<1 wt%) when compared to those from the Siele and Solforate mines where the Hg concentrations were up to 10 and 3 wt%, respectively. The first mining explorations in the Mt. Amiata district started in the mid-1800s and in 1899 the first flasks (about 34.5 kg) of liquid mercury were produced at ASSM. It is to mention that, according to historical records, Etruscans and Romans were using the Mt. Amiata cinnabar for decorative (cosmesis and painting) purposes (e.g. Sodo et al., 2008; Botticelli, 2019; Fantoni et al., 2022).

At the beginning of the past century, the exploration activity at ASSM was mostly focused along the large NE-SW-oriented Large Fracture (Forconi, 2011), which is likely crosscutting the thermal area of Bagni di San Filippo, Cipriana and Faggia (Municipality of Santa Fiora) (Fig. 1b). As suggested by Rimondi et al. (2015), Hg was likely transported to shallow crustal levels by the recent post-orogenic extensional tectonics (e.g., Brogi et al., 2011) and the Hg-rich mineralization was mostly located at the contact between the volcanic and the (impervious) sedimentary domains. In 1912, a NW-SE-oriented gallery was excavated (Galleria Indovina) close to the Indovina creek and Cipriana. This gallery was later connected to Galleria Cocca, where altered trachyte, with trace and veinlets of cinnabar, was found to follow the volcanic-(Eocene) sedimentary contact. Between 1914 and 1968, two major crises (before and after World War II, 1931 and 1948, respectively) decreased the mercury production. Afterward, new mine galleries were opened, and in 1956 four Gould furnaces were installed at ASSM to improve the technology for exploiting low-content mercury (ca. 0.3 wt%) ore. Between 1955 and 1965, the local mining company carried out an extensive survey in the Cipriana area, where the presence of cinnabar deposits was recognized, although mercury content was too low to be economically cultivable (Forconi, 2011). According to Dini (2017), at Cipriana, Decine and Sasseta scarcely Hg-mineralized fracture zones were present within the volcanic lithologies.

The production of liquid mercury at ASSM definitively shut down in

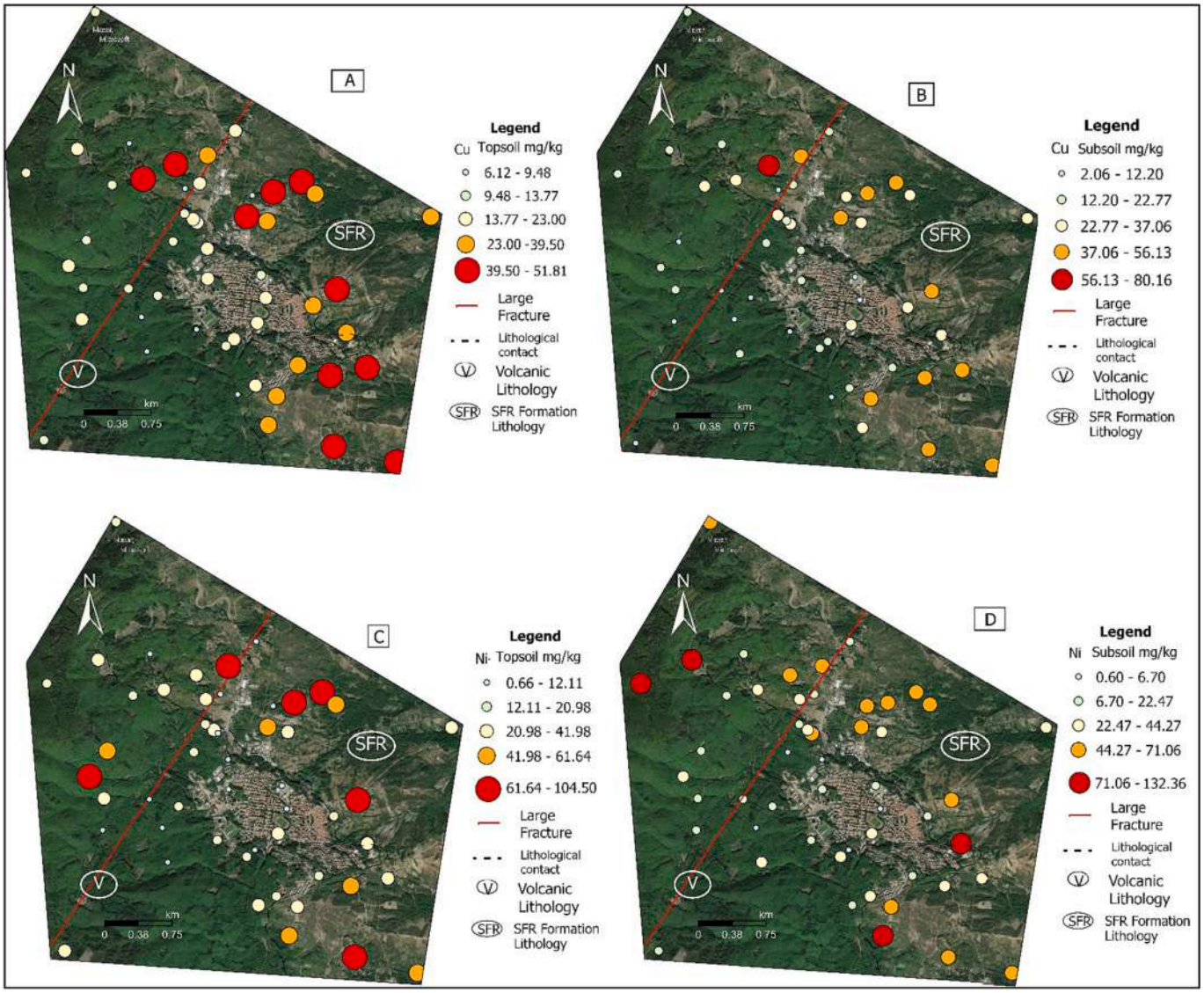

Fig. 6. Cu top-soil (A) and sub-soil (B) dot-maps; Ni top-soil (C) and sub-soil (D) dot-maps. Maxar, Microsoft indicates a high-resolution satellite and aerial imagery available on ArcGis-Pro 3.0. The dashed black curve represents the lithological contact between the volcanic and sedimentary domains, while the red line represents the Large fracture (Forconi, 2011). The concentration intervals are from the Fisher-Jenks classification. (For interpretation of the references to color in this figure legend, the reader is referred to the web version of this article.)

1982. The related mine tailings result to be distributed inside and outside the mining area. In 1942, several sites, mostly located in the western part of ASSM, were used to store the roasting material, e.g. Altone, Cachino, XXI, and the dumping areas 1, 2 and 3 and Le Lame (Fig. 2a). The Le Lame site became later on the most important storing site (Fig. 2b) and presently it covers an area of about 120,000 m^2 (Protano and Nannoni, 2018; Meloni et al., 2021 and references therein). According to Meloni et al. (2021), no information on when the tailings (locally named "*rosticci*") from the Gould and Cermak-Spirek furnaces operating at Abbadia San Salvatore started to be stored at Le Lame is available, although it may be hypothesized that this dump was active since the mid-1930s according to some local miners' reports.

3. Materials and analytical methods

3.1. Sampling strategy

From September 2021 to February 2022, 51 top-soils and 51 sub-soils from 10 to 50 cm and from 50 to 154 cm depth, respectively, were collected in the Municipality of Abbadia San Salvatore (Fig. 1b). The soil samples were taken from industrial, agricultural, residential, and wooded areas, following a twofold strategy: i) downtown the sampling density was more frequent, i.e. one sample each 300 to 600 m, with the aim to investigate the presence of mineralized areas, while ii) moving away from Abbadia San Salvatore the distance was increased up to 1500 m.

All soil samples were collected with a stainless-steel hand auger and stored in 1 L polyethylene containers before being transferred to the laboratory. In addition, seven rocks characterizing the study area were sampled, as follows: three volcanic rocks (OLF: olivine-latite lava flow, QRT: trachydacitic basal complex and VULC: Pianello *Fm*, following the classification of Conticelli et al., 2015), and four sedimentary rocks from the Ligurian Unit (SFR1, SFR2 and SFR3, belonging to the limestone member of Santa Fiora *Fm*, and APA, pertaining to the Argille a Palombini *Fm*). For each soil and rock site, the geographical coordinates (EPSG: 32632 - WGS84/UTM zone - 32N) were acquired with a Garmin GPS with an average error of 3 m. The soil and rock samples were oven-dried at 30 °C to avoid the release of gaseous mercury. Each sample was

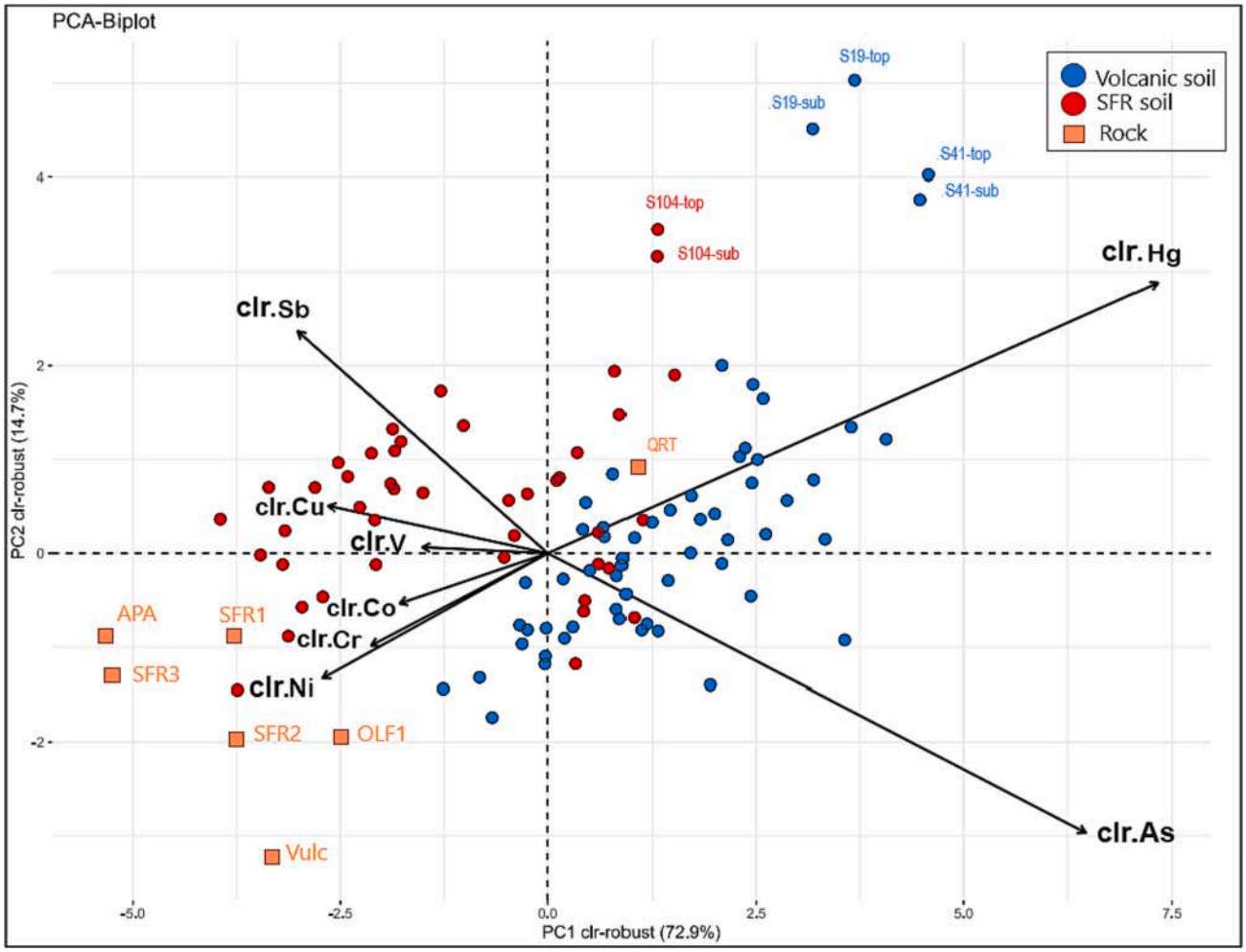

Fig. 7. Robust compositional biplot of the analyzed elements in both rocks and soils. The soil samples are divided according to the three dominant groups where they developed; blue circle: volcanic soils; red circle: SFR soils, and orange square: rocks. The variable labels in the biplot represent the clr-transformed data of the corresponding elements. (For interpretation of the references to color in this figure legend, the reader is referred to the web version of this article.)

then sieved at 2 mm according to the protocol adopted by Environmental Protection Agency of Tuscany (ARPAT) and described in Meloni (2022). The <2 mm fraction was then ground with a planetary mill (Pulverisette 5 Fritsch) equipped with agate mortars (250 mL) and balls before any mineralogical and chemical analysis.

The mineralogical composition was semi-quantitatively determined by X-Ray Diffraction (XRD) using a Cu-Kα radiation with D8 "Da Vinci" (Bruker) Diffractometer at the CRIST (Centro di Servizi di Cristallografia Strutturale) Laboratories (University of Florence).

Arsenic, Sb and Hg concentrations in soils and rocks were measured by ICP-MS (Agilent 7500 CE) at the accredited Laboratories of C.S.A. Ltd. (Rimini, Italy) according to the procedures outlined by EPA (U.S. Environmental Protection Agency): EPA 3051A 2007 + EPA 6010D 2018 for Arsenic and Antimony and EPA 7473 (2007) for mercury, respectively. Three replicates were performed for each sample and the error was <10 %. The concentrations of V, Cr, Co, Ni and Cu were measured by ICP-AES (Optima 8000) at the Department of Earth Sciences (University of Florence) after microwave (CEM MARS 5) digestion of 0.5 g powdered sample with aqua regia (7.5 mL of 30 % *v*/v HCl and 2.5 mL of 65 % v/v HNO_3) in PTFE bombs at 175 °C for 20 min. Quality control/quality assurance was evaluated by using international certified reference standards: 2709A Montana soil by NIST and JDO-1 GSJ rock. The difference between certified and recovered values was <10 %. The pH was measured in a soil-water suspension (1:5 *w/v* ratio) according to IRSA-CNR (1985) method via a bench pH-meter (Crison micro pH 2000) calibrated at pH = 4 and pH = 7 (Hanna standard solutions).

3.2. Statistical analysis

3.2.1. Descriptive statistics

The chemical data were statistically analyzed by using the software R and RStudio (R Core Team, 2021) and the summary exploratory statistics of the metal concentrations in soils was calculated. To perform all statistical calculations, the chemical data below the Limit Of Quantification (LOQ) (<1 mg/kg for all elements, and 0.005 mg/kg for Hg) were replaced with 2/3 of the LOQ itself (Gozzi, 2020; Gozzi et al., 2021). The ArcGis-Pro 3.0 software program was used to depict the dot-distribution maps that were prepared separately for top- and sub-soils.

3.2.2. Compositional data analysis

Multivariate methods in terms of the Principal Component Analysis (PCA) were applied to investigate the factors that control soil geochemistry (Ghezelbash et al., 2019) and identify pollution sources and anthropic contributions (Facchinelli et al., 2001). Rock and soil geochemical concentrations are compositional data since they represent proportions of a defined numerical total (e.g. mg/kg) (Buccianti and Pawlowsky-Glahn, 2005; Pawlowsky-Glahn and Buccianti, 2011; Filzmoser et al., 2018). Compositional data are vectors of always positive values that quantify the relative contribution of the D parts of the entire composition, consequently they only provide relative information. Their

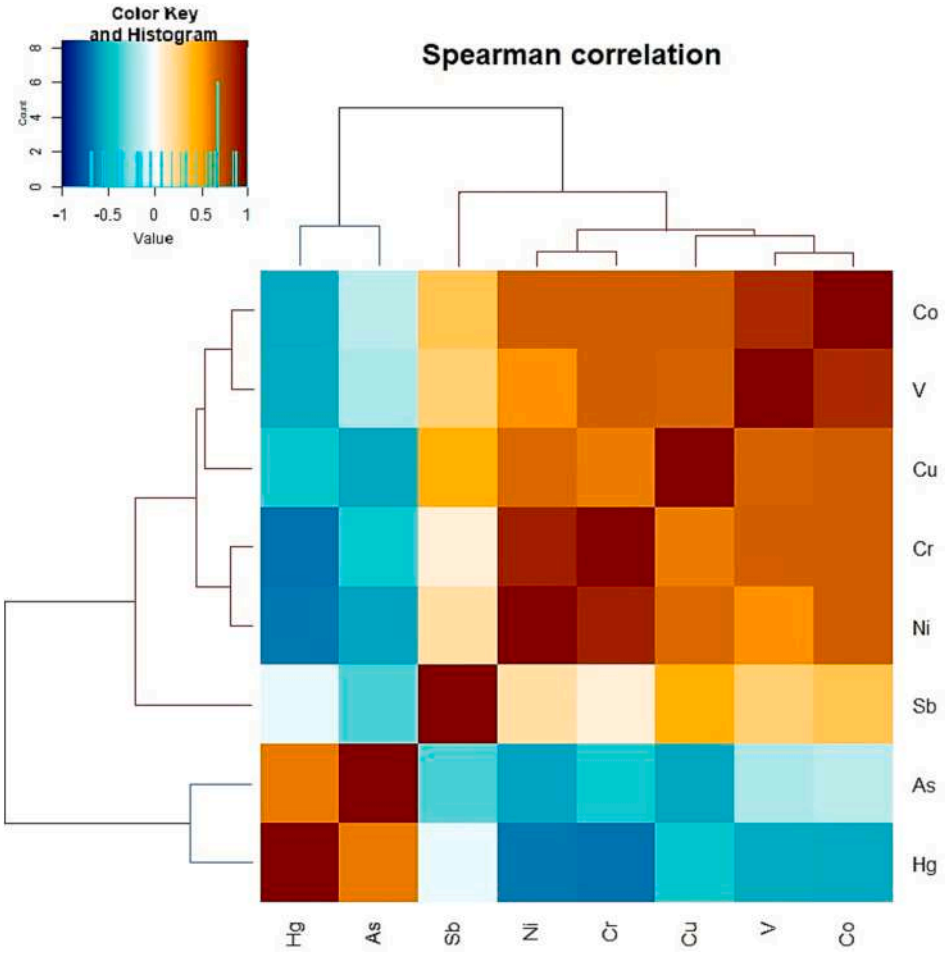

Fig. 8. Heatmap correlation for elements in soils based on clr transformation: blue colors indicate negative correlations, whereas red colors mark positive correlations. The color intensity shows the magnitude of the Spearman correlation coefficient. The blue lines in the dendrogram represent the Hg and As correlation in the volcanic lithology, whereas the red lines represent the correlation among the other elements in the SFR lithology. (For interpretation of the references to color in this figure legend, the reader is referred to the web version of this article.)

sample space, called *simplex* is governed by the Aitchison geometry that is based on perturbation and powering operations for moving points within the confined sample space (e.g. Pawlowsky-Glahn and Egozcue, 2001). To solve problems related to the numerical constraint, data placed in the simplex are transported to real space using transformations (e.g. isometric log-ratio (ilr) and centered log-ratio transformation (clr), proposed by Egozcue et al. (2003) and Aitchison (1986), respectively). The transformed data can properly be analyzed using traditional statistical methods, including multivariate techniques (Pawlowsky-Glahn and Egozcue, 2020), with some attention for the clr transformation, due to the zero sum restriction. In particular, clr transformation divides each term of a composition by the geometric mean of all the considered parts. Thus, the obtained clr coordinates link each element to the barycenter of the entire soil composition (Gozzi et al., 2020 and references therein), and are to be interpreted in terms of relative changes.

In this work, the robust PCA (rPCA), according to Filzmoser et al. (2009) was applied. The rPCA was performed using the R library "robCompositions" (Templ et al., 2011), where the data were back-transformed to clr coefficients after being transformed with the ilr before doing the rPCA. Successively, the resulting scores and loadings were used as input factors within the R package Factoextra (Kassambara and Mundt, 2019) for a better visualization of the outputs (Gozzi et al., 2021).

Spearman correlation on clr-transformed data, following the method described by Kynčlová et al. (2017) and Reimann et al. (2017), was used for the correlation analysis among metals soils since it is relatively robust against data outliers (Reimann et al., 2017). Spatial distribution maps of the clr-transformed data, constructed with Ordinary Kriging, were prepared separately for top- and sub-soils and visualized with the ArcGis-Pro 3.0 software package. Additionally, spatial distribution maps of PC scores were also constructed with Ordinary Kriging. The reliability of the mathematical models was tested by cross-validation, a procedure that uses the variogram model to recalculate each measurement. The spatial behavior was modeled by using an omnidirectional variogram. Further information on variogram parameters can be found in Section 5.1 for PCA scores and Section 5.2 for clr-maps.

3.2.3. *Determination of geochemical baseline*

Following a consolidated classical approach (Turkey, 1977; Gilbert, 1987), the baseline values were defined for the different groups of data according to i) the geological map, to divide the volcanic and sedimentary domains and ii) the top- and bottom (or sub-) soils. The baseline was computed by using the ProUCL 5.2.0 software (Singh and Maichle, 2015), allowing to calculate different background/baseline values according to the type of dataset distribution (e.g. normal, lognormal, gamma and non-parametric), but a 95 % one-side upper tolerance limit (ULT) with 95 % coverage (UTL95-95) was of greatest interest (Crane et al., 2021). The software requires a minimum of eight detected sample results (Singh and Maichle, 2015). In each computed geochemical baseline, the type of distribution (e.g. normal, gamma, log-normal or non-parametric) was determined. According to Crane et al. (2021) and Singh and Maichle (2015), the UTL95-95 value based on a normal

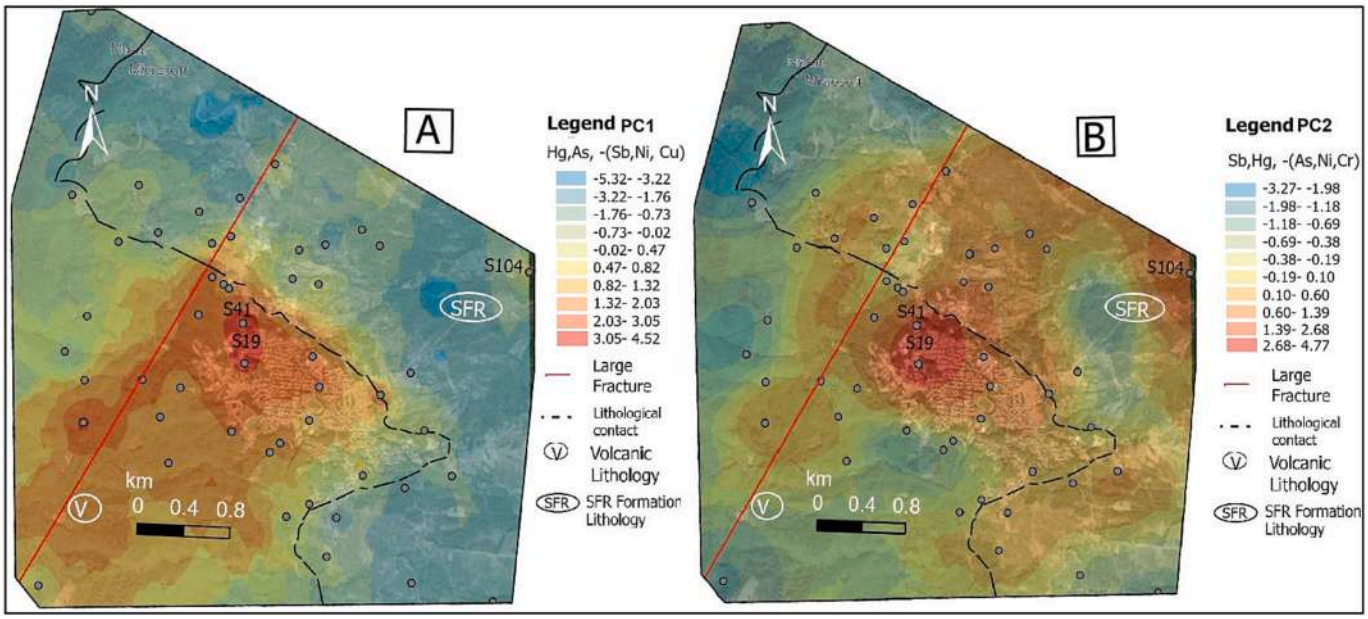

Fig. 9. Distribution of component scores for (a) PC1 and (b) PC2 element associations. The maps represent the total of loading but only report the main ones (>−0.5). The sign "–" in front of the bracketed elements represent the negative scores in the two high scores Maxar, Microsoft indicates a high-resolution satellite and aerial imagery available on ArcGis-Pro 3.0. The red line is the Large Fracture (Forconi, 2011), the dashed black curve represents the lithological contact between the volcanic and sedimentary domains. (For interpretation of the references to color in this figure legend, the reader is referred to the web version of this article.)

distribution was of utmost priority to employ. The Wilson Hilferty (WH) and Hawkins Wixley (HW) methods were used to estimate the gamma UTL95-95 upper limits when the data were not normally distributed, and the gamma distribution was employed. The non-parametric result was applied when the data followed neither a normal nor a gamma distribution. Singh and Maichle (2015) do not recommend the use of log-normal UTL95-95 values because unstable and unrealizable huge numbers based on a log-normal dataset are provided (Singh and Maichle, 2015). If non-parametric results could not be applied, graphic methods were then used as suggested by SNPA (2017). Using graphical methods (e.g. Q-Q graph, box-plot) and specific hypothesis tests, the ProUCL software allowed to identify the presence of outliers.

4. Results

4.1. Mineralogical composition

The mineralogical data of rock and top- and sub-soil samples are listed in Tables S1, S2, and S3 (Supplementary Materials S1, S2 and S3), respectively. In the SFR1, SFR2, SFR3, APA, and QRT samples, the latter being characterized by secondary calcite as the main component, quartz and phyllosilicates were found while plagioclase was sporadically present. In the SFR3 rock, ankerite and chalcopyrite were occurring in trace. VULC and OLF1 were mostly dominated by K-feldspar and plagioclase and subordinate phyllosilicates and pyroxene.

In the soils, quartz and phyllosilicates, including clay minerals and micas, were the main minerals, while K-feldspar and plagioclase were subordinate. Calcite was present in the sedimentary lithologies as a minor component. Occasionally, primary minerals such as pyroxene, amphibole and hematite were recorded. Gypsum was only found in S16 (sub-soil).

4.2. Descriptive statistics of PTEs: rocks, top-soils and sub-soils

Geographic coordinates, pH values and concentrations of Hg, As, Sb, Cr, Cu, Co, V, and Ni (in mg/kg) of the seven analyzed rocks are listed in Table 1, where the mean values of sandstone, limestone and sialic rocks from the literature are also reported for comparison. The pH varied from alkaline for the carbonate (SFR1, 2, and 3) and siliciclastic (APA) rocks, to weakly acidic to acidic for the magmatic rocks. The metal concentrations were variable: the lowest content of Hg was found in SFR1, 2, and 3 and APA (<0.015 mg/kg), whereas QRT showed a concentration of 0.68 mg/kg. Arsenic in the volcanic rocks (VULC, OLF1, and QRT) was between 6 and 13 mg/kg, while it clustered around 1.0 mg/kg in the sedimentary rocks. Antimony had a maximum concentration in the sedimentary rocks (APA and SFR), while it was always <1.0 mg/kg in the volcanic rocks. Chromium, Cu, Co, V, and Ni showed comparable concentrations for both the sedimentary (from 33.6 to 75.2 mg/kg, from 23.0 and 67.8 mg/kg, from 4.7 to 7.7 mg/kg, from 31.8 to 85.5 mg/kg and from 24.2 to 89.8 mg/kg, respectively) and volcanic (from 39.5 to 94.5 mg/kg, from 49.0 to 49.3 mg/kg, from 14.6 to 18.4 mg/kg, 62.6 to 82.5 mg/kg and 42.8 to 64.9 mg/kg, respectively) rocks, with the exception of SFR and QRT, whose contents were significantly lower than the other rocks for most PTEs.

The arithmetic mean concentrations of PTEs of the sialic rocks analyzed in this study (Table 1) were higher than those reported for Cr (Condie, 1993), Sb (Gao et al., 1998), As (Geochemical Earth Reference Model (GERM) Reservoir Database; Staudigel et al., 1996), Ni, V and Co (Kemp and Hawkesworth, 2004), and Hg (Reimann and de Caritat, 1998). The mean concentrations of Sb, Co, V and Cr in the limestone resulted to be higher than those proposed by Gao et al. (1998). Similarly, Cu and Ni showed mean contents greater than those recorded by Reimann and De Caritat (1998) and Salminen et al. (2005), respectively. On the other hand, the As mean concentration was in agreement with that proposed by Staudigel et al. (1996). Only the Hg mean concentrations in limestone resulted to be lower than those listed by Gao et al. (1998). The PTEs concentrations in the APA rock were lower than those proposed by different authors (Table 1), with the exception of Sb, whose content was higher than those reported by Gao et al. (1998).

In Tables 2 and 3, the main descriptive statistics of the pH values and the concentrations of PTEs from the 51 top- and 51 sub-soils (e.g. minimum, maximum, mean, median, standard deviation, and skewness) are listed, respectively. The full dataset is reported in the Supplementary Material 4 and 5 (Tables S4 and S5 for top- and sub-soils, respectively). The top-soil samples showed slightly acidic pH values whereas those of sub-soils were mostly circum-neutral (Table 2). Generally speaking, Hg,

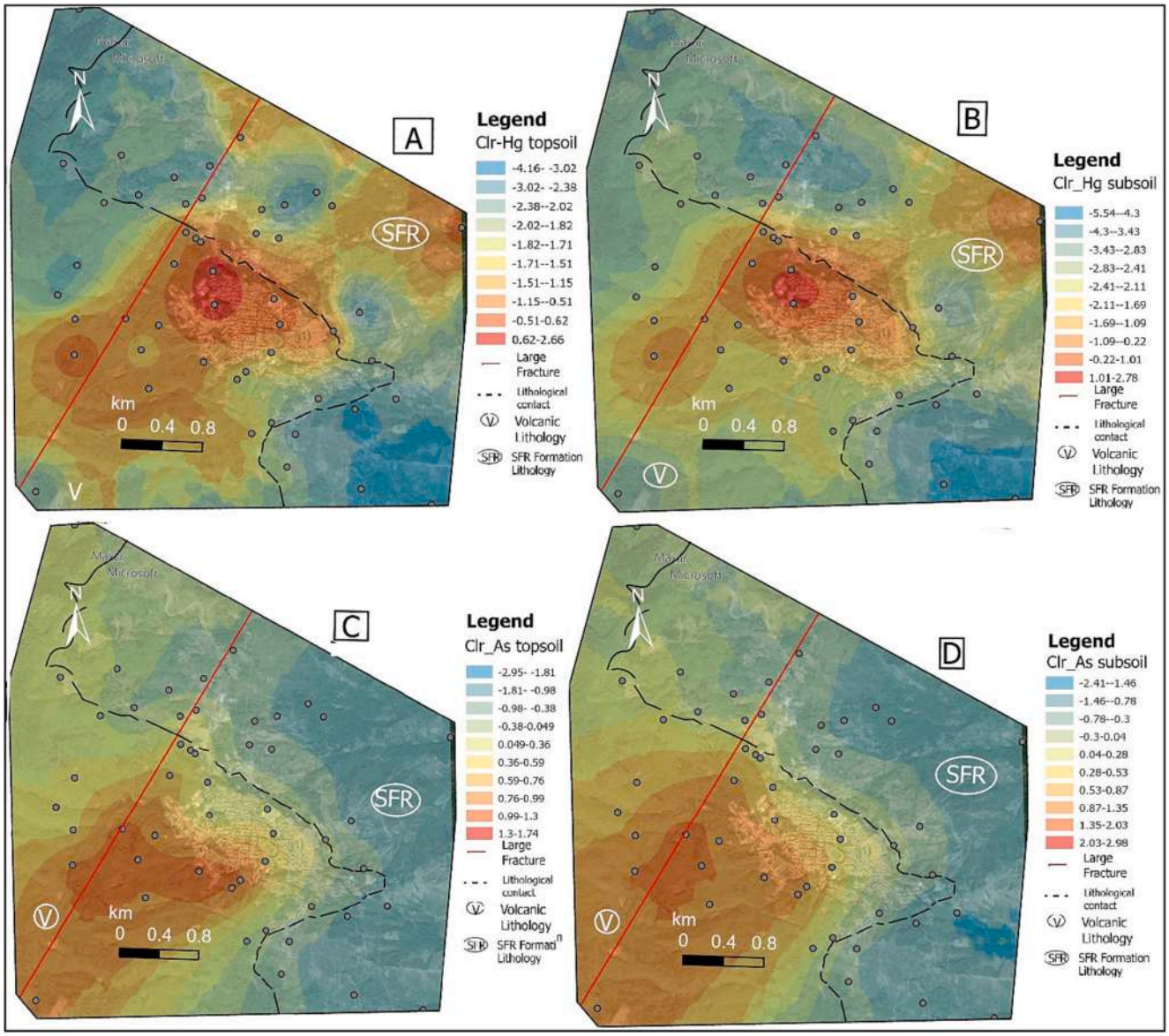

Fig. 10. A) Hg Geographical distribution maps clr-transformation data top-soil; B) Hg Geographical distribution maps clr-transformation data bottom-soils; C) As Geographical distribution maps clr-transformation data top-soil; D) As Geographical distribution maps clr-transformation data bottom-soils. Maxar, Microsoft indicates a high-resolution satellite and aerial imagery available on ArcGis-Pro 3.0. The dashed black curve represents the lithological contact between the volcanic and sedimentary domains, while the red line represents the Large fracture (Forconi, 2011). (For interpretation of the references to color in this figure legend, the reader is referred to the web version of this article.)

Ni, As, and Sb in the top-soils had largely variable concentrations, since they were spanning from two to three orders of magnitude (from 0.16 to 211 mg/kg, from <1 to 104.5, from <1 to 63.8 mg/kg and from <1 to 12.0 mg/kg, respectively), while Cr, Cu, Co, and V were varying within one order of magnitude (from 11.8 to 157.5 mg/kg, from 6.1 to 51.8 mg/kg, from 1.8 to 22.1 mg/kg and from 13.6 to 148.9 mg/kg, respectively). Such a heterogeneous distribution of the PTEs contents was also observed for the sub-soils: As, Sb, and Ni were indeed ranging within three orders of magnitude. Differently, Cr, Cu, Co, and V were spanning within one order of magnitude. It is to point out that the concentration of Hg showed the largest variations since it was comprised within four orders of magnitude (from 0.03 to 268 mg/kg).

By comparing the results of the eight analyzed elements (Tables S4 and S5) with those imposed by the Italian Law (Legislative Decree 152/06; Lgs.D. afterwards), 45 % and 33 % of top- and sub-soil samples presented Hg concentrations higher than those for areas intended for residential use (1 mg/kg), whereas approximately 25 % of both top- and sub-soil showed Hg concentrations higher than those for areas intended for industrial use (5 mg/kg). Regarding As, approximately 25 % of both top- and sub-soil had concentrations higher than those for areas intended for residential use (20 mg/kg), while <10 % were above the limit for industrial use (50 mg/kg). As far as Sb is concerned, only one sample from the top-soil (S19) showed concentration above the law limit for areas destined to residential use (10 mg/kg), while in the sub-soils a concentration above the law limit for areas of industrial use (30 mg/kg) was recorded. Cobalt, Cr, and V showed exceedances in 3, 1, and 12 top-soil samples out of 51, and in 5, 4, and 13 sub-soil samples out of 51 for areas intended for residential use (20, 150, 90 mg/kg, respectively). Nickel showed 2 sub-soil samples with a concentration higher than the limit for soils intended for residential use (120 mg/kg). Finally, the concentrations of Cu were systematically below the law limits.

According to the data reported in Tables 2 and 3, except for those of Co in the top-soils, the significant difference between mean and median values is indicative of a non-normal behavior and a right-skewed

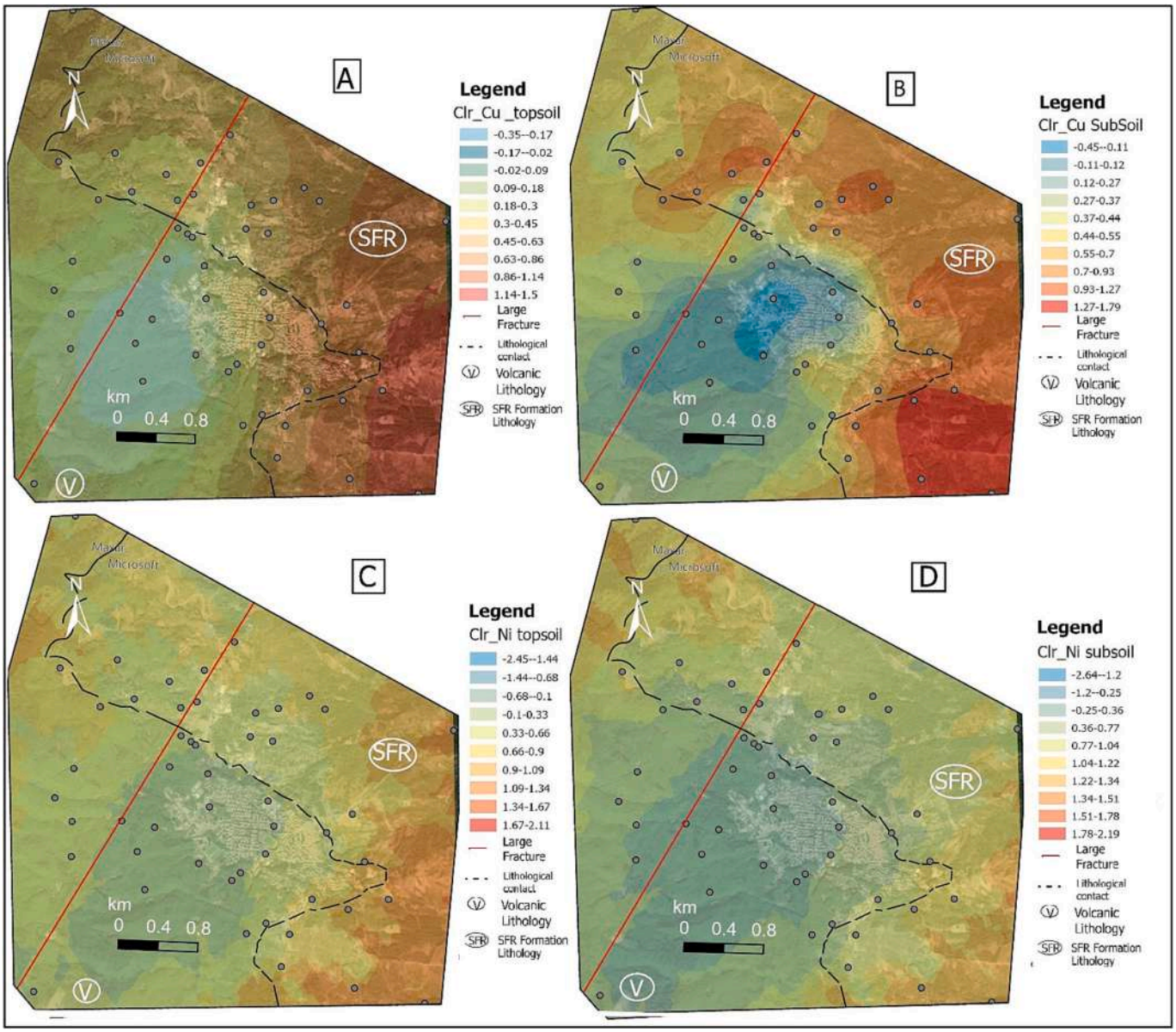

Fig. 11. A) Cu Geographical distribution maps clr-transformation data top-soil; B) Cu Geographical distribution maps clr-transformation data bottom-soils; C) Ni Geographical distribution maps clr-transformation data top-soil; D) Ni Geographical distribution maps clr-transformation data bottom-soils Maxar, Microsoft indicates a high-resolution satellite and aerial imagery available on ArcGis-Pro 3.0. The dashed black curve represents the lithological contact between the volcanic and sedimentary domains, while the red line represents the Large fracture (Forconi, 2011).

Table 4
Type of distribution, proposed geochemical baseline value (UTL95-95), 95th and 99th percentile of Hg, As, Cr and V in the volcanic top- and sub-soils without outliers. N: normal distribution; LN: log-normal distribution; G: Gamma distribution.

	Volcanic top-soil				Volcanic sub-soil			
	Type of distribution	UTL95-95	95th percentile	99th percentile	Type of distribution	UTL95-95	95th percentile	99th percentile
Hg	LN/G	19.3	12.3	18.9	LN/G	20.6	12.9	20.9
As	LN/G	77.4	58.2	79.4	LN/G	87.0	65.5	90.1
Cr	N/LN/G	89.9	77.5	91.5	N/LN/G	100.6	85.4	102.2
V	N/LN/G	95.2	83.3	97.1	N/LN/G	95.4	84.1	97.3

distribution for most elements (Fig. 3A and B for top- and sub-soils, respectively).

Breaking down the concentrations of the elements on a lithological basis, the largest variability in terms of Hg and As is observed for the volcanic soils. Vice versa, the other elements are more variable in the sedimentary domain (SFR soils). The box-plots of the Hg and Sb concentrations (in mg/kg), transformed into logarithmic values to better appreciate their variability, are reported in Fig. 4. The concentrations of Sb, Cu, Co, V, Ni and Cr in the analyzed rocks mostly cover the wide range related to the top- and sub-soils for both lithologies (Fig. 4). On the other hand, the As distribution of the investigated rocks is partly overlapping that of the SFR (limestone/siliciclastic) soils, while it only

Table 5
Type of distribution, proposed geochemical baseline value (UTL95-95), 95th and 99th percentile of Hg, As, Co, Cr and V in SFR top- and sub-soils without outliers. N: Normal distribution LN: log-normal distribution; G: Gamma distribution.

	SFR top-soil				SFR sub-soil			
	Type of distribution	UTL95-95	95th percentile	99th percentile	Type of distribution	UTL95-95	95th percentile	99th percentile
Hg	G	7.5	5.0	7.6	LN/G	7.2	4.0	6.6
As	LN	36.7	18.3	34.4	LN	41.6	20.4	38.5
Ni	N	110.1	90.9	109.5	N	84.8	72.1	83.6
Co	N	24.8	21.6	24.6	N	25.92	22.7	25.7
Cr	N	178.0	149.5	177.1	N	174.7	147.7	172.2
V	N	166.2	142.1	165.5	N	175.9	150.5	175.1

Table 6
The range values of the proposed geochemical baseline (in mg/kg) for Hg, As in volcanic lithology and Hg, As, Co, Ni, Cr and V in SFR lithology. The last column lists the reference values for each HM according to the Lgs.D.

	Volcanic top-soil	Volcanic sub-soil	SFR top-soil	SFR sub-soil	Lgs. D.
Hg	17.3–21.2	18.5–22.7	6.8–8.3	6.5–7.9	1
As	69.6–85.1	78.2–95.6	Lgs.D.	Lgs.D.	10
Co			22.3–27.2	23.3–28.5	20
Ni			Lgs.D.	Lgs.D.	120
Cr	Lgs.D.	Lgs.D.	160.2–195.8	157.2–192.2	120
V	85.7–104.2	85.9–104.9	149.6–182.8	158.3–193.5	90

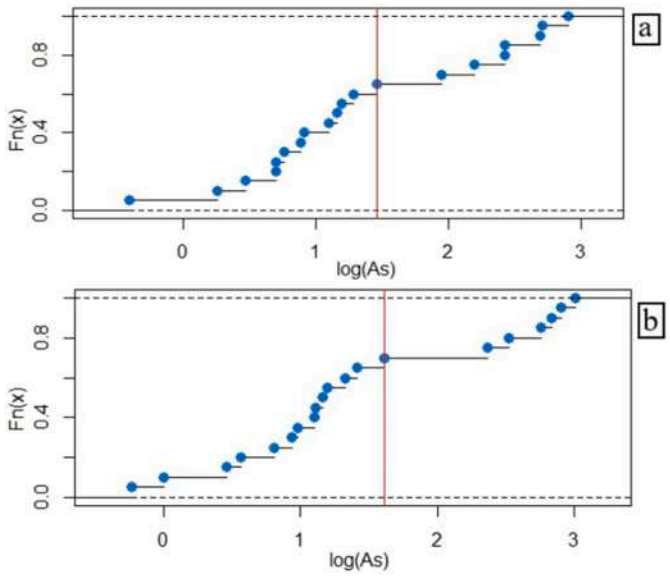

Fig. 12. CP-plot of As in SFR top- (a) and sub- (b) soils. The red line represents the logarithmic baseline value: 1.46 (4.3 mg/kg) and 1.61 (5.0 mg/kg) for top- and sub-soils, respectively. (For interpretation of the references to color in this figure legend, the reader is referred to the web version of this article.)

covers the lower contents of those developed on the volcanic lithology. It is to note that the Hg concentrations in rocks were significantly lower than those of soils, with the exception of QRT (Hg content of 0.68 mg/kg), suggesting that mercury was likely enriched by the hydrothermal alteration suffered by this sample. In order to have a first spatial visualization of the data and to better evidence the results derived by the box-plots, dot-maps of the individual elements were built, as follows: Hg, As, Cu, and Ni in the top- and sub-soils are presented in Figs. 5A and B, C and D, 6A and B, and C and D, respectively, while those of Sb, Cr, Co, and V (top- and sub-soils) are reported in the Supplementary Material S6.

Figs. 5 and 6 allow to evidence that Hg and As are mainly enriched in the soils developed on the volcanic lithology with respect to those formed on the sedimentary cover. Vice versa, Cu and Ni (as well as Sb, Co, Cr, and V, see Supplementary Material S6) tend to be enriched in the SFR lithology. Basically, the dot-maps fully support the subdivision highlighted in Fig. 4. When considering the soil samples collected close to or at the contact between the volcanic and sedimentary domains, relatively high contents of PTEs were determined. This could be related to either the presence of volcanic and/or sedimentary slope deposits overlapping each other or not well-defined geological limits.

5. Discussion

5.1. Compositional data analysis of PTEs in rocks, top-soils and sub-soils

In order to evaluate the lithological subdivision, previously adopted in Fig. 4, a non-parametric test called log-contrast homogeneity test (lc test), available on R package composition (Palarea-Albaladejo and Martin-Fernandez, 2015), was applied on ilr-transformed data. The test confirmed the results of the previous subdivision (Paragraph 5.1), i.e. top- and sub-soil have no significant differences in both mean and variance, the test showing a *p-value* > 0.05, whereas they are relevant when the volcanic and SFR lithologies, with *p-value* < 0.05, are considered.

Therefore, after analyzing the individual variables in a classical statistical framework, with the aim of investigating the variance-covariance structure of the data by maintaining the lithological subdivision, a rPCA (also including the rock chemistry), which implies the transformation of the data by using the ilr transformation, can be applied (Fig. 7), where the top- and sub-soils are regarded as a unique population. According to Boente et al. (2018), the PCA result leads to recognize the most relevant - associations in a compositional dataset. The variability of each clr-variable, in the biplot, is proportionally related to the lengths of the arrows and attention is paid on the links between their vertices (Daunis-I-Estadella et al., 2006), and the variation of single elements are referred to the compositional barycenter. Hereafter the single element clr-variable will be indicated clr. followed by the symbol of the element (e.g. clr-Hg, clr.As). The first component (PC1) accounts for 72.9 % of the total variability, while the second one (PC2) explains 14.7 % (Fig. 7). clr.Hg and clr.As provide the main contribution to the first component (positive loadings), while clr.Sb, clr.Cu, and clr.Ni oppose on negative loadings with a more subordinate contribution, with respect to the compositional barycenter. In particular, the clr.Cr, clr.Co, clr.Cu, clr.Ni, and clr.V have shorter rays and tighter links, showing a similar pattern of variability (Fig. 7). On the other hand, it is possible to recognize that three groups of samples can be distinguished by the vectors of clr.Hg vs. clr.Ni, clr.Cr and clr.Co, while the volcanic and SFR soils can also be differentiated by the vectors of clr.As vs. clr.Sb. The second component (PC2) is mainly represented by clr.Hg and clr.Sb (positive loadings), whereas the clr.As provides the main contribution on negative loadings, followed by clr.Ni and clr.Cr. The QRT sample is the only rock showing a different behavior with respect to the other rock samples (Fig. 7).

This agrees with both the results of the mineralogical analysis, which revealed a hydrothermally altered volcanic rock characterized by the

presence of secondary calcite, and those of the univariate statistics (Fig. 4). To further validate the lithological subdivision, previously obtained with the lc test, a heatmap correlation for compositional data, based on the non-parametric Spearman correlation coefficient, is built following the method described by Kynčlová et al. (2017) and Reimann et al. (2017) (Fig. 8). This method creates orthonormal coordinates for which standard correlations are generated by considering all the relative information of two variables (compositional parts) with respect to the remaining variables. The process is repeated for each pair of variables, and the results can conveniently be represented by a "heatmap", which is a hierarchical clustering algorithm that reorders the chemical variables according to each other existing similarity. Due to the extremely effective and thorough graphical portrayal of all relationships in the heatmap, this approach was chosen over that suggested by Aitchison (1982). The heatmap shows two associations of variables similar to those depicted by PCA: i) Hg and As; ii) all others elements. In order to better interpret the results of the rPCA, the spatial distribution of the component scores of PC1 and PC2 are reported in Fig. 9. The nugget effect of PC1 and PC2 represents 0 % and 19 %, respectively, of the global variance (nugget + sill). This suggests that the data are highly spatially autocorrelated at larger scales and random fluctuations at very fine scales can be regarded as negligible when compared to the dominant structure or geology at larger scales.

By observing the distribution map of the PC1scores (Fig. 9a), it can be seen that the high positive scores are mostly distributed in the western part of the study area. This is due to the presence of volcanic lithologies in which Hg (Tanelli, 1983) and As mineralization have been found in association with non-economic minerals (Rimondi et al., 2015). In the eastern area, the scores are negative due to the presence of SFR lithologies. Therefore, PC1 could represent the contribution of volcanic vs. SFR lithologies. The high values of PC2 scores (Fig. 9b) are mainly in association with the SFR lithologies, whereas they are low for the volcanic rocks, with exception of two samples in the northern part of Abbadia San Salvatore (S19 and S41, Fig. 9a), which also have major values in PC1. These two samples in the rPCA (Fig. 7) are outliers as well the S104 sample.

5.2. Spatial distribution patterns of the clr-transformed data

Single-component geochemical thematic maps are commonly used in regional geochemical surveys to offer more specific information on the spatial distribution of elements and identify their potential geogenic or anthropogenic sources (Reimann et al., 2012; McKinley et al., 2016; Sahoo et al., 2020). The clr-distribution maps are more useful than the raw distribution maps to understand the general trend of the geochemical process, because they avoid the "weakness" of the raw data and take into account the relative compositional changes (Reimann et al., 2008). According to Reimann et al. (2012) and McKinley et al. (2016), the maps of the clr-transformed variables represent a relative abundance of the element with respect to the geometric mean of all measured elements. In this study, the maps report clr-transformed variables constructed to understand how the considered element behaves with respect to barycenter of the composition. The main parameters of the variogram model are listed in the Supplementary Material S6 (Table S7). The nugget effect in all clr-variables in topsoil showed a low variation from 0 % up to 38 % of global variance, showing strong spatial autocorrelation at a large scale with a predominant geological structure driving the variability of the data, with except of clr.Ni. On the other hand, clr.Ni in top soil and clr.Hg, clr.As, clr.Ni and clr.Cr in subsoil showed a 47 %, 40 %, 47 %, 45 % and 44 % of global variance, respectively, suggesting very small-scale variation (e.g. mineralization) with larger-scale geological influences contributing considerably to the overall variability of the data The clr-maps show that the underlying bedrock geology (parent lithologies), rather than anthropogenic causes, controls most components in both the top- and sub-soils. The clr-maps of Hg are reported in Fig. 10. The clr.Hg tends to increase in both the top- and sub-soils along a NE-SW orientation, indicating a greater importance of Hg relatively to the compositional barycenter. This is in agreement with the main structural directions (Brogi and Liotta, 2017) that coincide with those of the main normal faults (Liotta, 1991; Martini and Sagri, 1993; Brogi et al., 2010; Vezzoli and Principe, 2023) and related structures (Brogi et al., 2010; Vezzoli and Principe, 2023) (Fig. 1), and the Hg-rich ore deposits belts described by Brogi et al. (2011). When comparing the main trend of a possible fault system, governing the Hg distribution pattern, as suggested by Forconi (2011) (Fig. 1), with respect to that evidenced in Fig. 10, a slightly shifted toward NNW-SSW is highlighted. Fig. 10 is also in agreement with the PC1 map distribution, and high values of clr.Hg are represented by the S41 and S19 samples (volcanic lithology), and S104 top- and sub-soils (SFR lithology). In the rPCA (Fig. 7), these three top- and sub-soil samples are to be regarded as outliers. Sample S41 is located near the Zampa della Mula area, where Hg concentrations were up to 0.2 % (Forconi, 2011), while sample S104 is located near an exploratory geothermal well. Thus, the elevated clr.Hg values in these samples could be associated with highly mineralized areas. These observations also confirm the Hg range concentrations analyzed by Ferrara (1999) in the eastern slope of the Mt. Amiata. Concerning the S19 sample, by comparing the location of this sample with the old mining dumps (Fig. 2a), it can be noticed that it is situated in an old, not previously recorded, mining dump. This observation can also explain the high content of Sb in the sub-soil sample (109 mg/kg), as also highlighted in dot-maps (Supplementary Material S6). Antimony was scarcely present in the AAS mines, while it was more abundantly occurring in other Mt. Amiata mines (e.g. Morone: up to 1.5 wt% Sb, Dini, 2017; Bagnore and Siele: Brogi et al., 2011, Rimondi et al., 2015) whose ore deposits were also treated at AAS mining plant. This is also in agreement with the chemical composition of the mining waste stored in the Le Lame mining dump (Meloni et al., 2021), although the recorded concentrations of Hg, As and Sb were here significantly lower than those measured in the S19 sample. The fact that this material belongs to mining dumps is further highlighted by XRD analyses. The main component in this soil was indeed calcite, representing the main component of the gangue (Rimondi et al., 2015) of the Mt. Amiata mining dumps. As evidenced in Fig. 10A, the clr.Hg values in the topsoils tend to be slightly higher than those measured in the sub-soils (Fig. 10B). This can possibly be associated with an anthropogenic influence due to the past mining activity or Hg occurring in the litterfall that constitutes a significant amount of Hg dry deposition in forested areas of terrestrial ecosystems (Risch et al., 2012 and references therein).

The distribution pattern of clr.As (Fig. 10) perfectly overlaps the Mt. Amiata volcanics, which are characterized by high As contents when compared to the soils developed on the sedimentary formations. The distribution pattern maps of clr.Cu and clr.Ni are shown in Fig. 11 A and B and C and D, respectively, whereas those of clr.Sb, clr.Co, clr.V and clr.Cr are reported in the Supplementary Material S6. Their distribution is mostly controlled by the sedimentary lithology, and they showed the presence of more positive values in the northern portion of the Mt. Amiata volcanic rocks.

5.3. Determination of geochemical baseline values with ProUCl 5.2.0 software

One of the aims of this work was that to compute the geochemical baseline values of the analyzed chalcophile and siderophile elements. The environmental authorities require that these values are to be calculated by using the ProUCl software. This implies the use of the raw dataset, allowing to compare our results with those reported in the Lgs. D.

According to Reimann and de Caritat (2005), the term "natural background" refers to the elemental "background" value and reflects natural processes unaffected by human activities. In the study area, the Hg mine has been exploited since the Etruscan and Roman times,

therefore, discriminating the natural component from an anthropic source is rather complicated. Consequently, for the studied soils it was decided to compute a geochemical baseline value, which for any element is defined as both the concentration of the natural background and that due to an anthropogenic contribution. The geochemical baseline only applies to those elements that have at least one sample with concentrations higher than the limit for areas to be destined to public green, in agreement with the Lgs.D. According to Salminen and Gregorauskiene (2000), Sahoo et al. (2020) and Cicchella et al. (2022), concentrations of PTEs in soils are strongly depending on the bedrock lithology. Consequently, as previously discussed, significant differences between volcanic and SFR soils were recorded. Therefore, the dataset was divided in two sub-datasets: i) volcanic top- and sub-soils and ii) SFR top- and sub-soils. From each of them, the potential outliers were removed after the outlier tests and their individuation in the Q-Q plots and box-plots. The proposed geochemical baseline values (UTL95-95), computed for the volcanic (Hg, As, Cr, and V) and SFR (Hg, As, Ni, Co, Cr, and V) soils, the type of distribution, and the 95th and 99th percentile of the distribution without outliers, respectively, are reported in Tables 4 and 5. When the distribution is both log-normal and gamma, the UTL95-95 of gamma distribution was selected.

According to Reiman and de Caritat (2017) and Santos-Francés et al. (2017), the geochemical background/baseline values are to be referred to a range of concentrations for a specific area, being the use of a single value affected by an analytical uncertainty. In our case, we decided to apply a confidence interval of ±10 % to the proposed geochemical baseline value for the heavy metals from the Municipality of Abbadia San Salvatore, this uncertainty basically reflecting the analytical error with respect to the international standard samples analyzed along with the studied samples. Thus, the new proposed geochemical baseline values for the PTEs with respect to those previously computed are summarized in Table 6.

Therefore, considering the confidence interval, the geochemical baseline values of Hg in the volcanic top- and sub-soils are between 17.3 and 21.2 mg/kg and 18.5–22.7 mg/kg, respectively (Table 6). The geochemical baseline ranges for As and V in volcanic soils are higher than that of Hg, being of 69.6–85.1 mg/kg (top-soils) and 78.2–95.6 mg/kg (sub-soils), and 85.7–104.2 mg/kg (top-soils) and 85.9–104.9 mg/kg (sub-soils), respectively (Table 6). According to the ProUCL 5.2 software, Cr in volcanic soils (80.9–98.9 mg/kg in top and 90.5–110.6 mg/kg in sub soils) does not break through that indicated by the Lgs.D. (120 mg/kg) (Table 6).

The geochemical baseline ranges for Hg, Co, Cr and V in the SFR top- and sub-soils (Table 6) are, as follows: 6.8–8.3 mg/kg and 6.5–7.9 mg/kg; 22.3–27.2 and 23.3–28.5 mg/kg; 160.2–195.8 mg/kg and 157.2–192.2 mg/kg and 149.6–182.8 mg/kg and 158.3–193.5 mg/kg, respectively. Nickel results to be lower than the reference values reported by the Lgs.D.: 91.2–111.5 mg/kg (top-soils) and 76.3–93.2 (sub-soils) mg/kg.

As reported in Table 5, the concentrations of As in the SFR top- and sub-soils have a log-normal distribution and, as previously described, graphical methods can be adopted to verify the baseline obtained by ProUCL. A Cumulative Probability diagram (CP-plot) can thus be built without including the outliers. The operator evidences whether a break of slope on the CP-plot diagrams is present, thus allowing to identify a specific threshold (Cave et al., 2012; Johnson et al., 2012; Reiman and de Caritat, 2017). The CP-plots of the As log-value in the SFR top- and sub-soils are shown in Fig. 12, respectively. The red line refers to the value where a slope break occurs and represents the suggested geochemical baseline value. Since the values are logarithmic, these were then back-transformed to obtain the final value, i.e. 4.3 and 5.0 mg/kg, for top- and sub-soils, respectively, which are lower than those proposed by the Lgs.D. for areas destined to public green (10 mg/kg). When comparing these two concentrations with those calculated by ProUCL (Table 5), the UTL95-95 values are significantly higher than those computed with the graphical method, highlighting an error in the attribution of the geochemical baseline or background value in a log-normal distribution, especially for data showing a standard deviation <1 and a dataset consisting of <30–50 values (Singh and Maichle, 2015).

6. Conclusions

The concentration intervals of the investigated PTEs from the top- and sub-soils, developed on the volcanic and sedimentary formations adjacently the former mining area of Abbadia San Salvatore (Mt. Amiata, Siena, Southern Tuscany), were defined with the use of classical statistical methods and interpretation of the variance-covariance structure improved with the use of a compositional approach. According to the clr distribution maps, the parent lithology, rather than an anthropogenic contribution, is governing the distribution of most elements in the studied soils, despite the depth from where they were collected. The resulting rPCA application, associated with the geological features, indicates that the geochemical variability is dominated by Hg and As clr-variables and is intimately related to the area where the volcanic products are distributed and, likely, to the presence of Hg-mineralization. Nevertheless, the proximity to the former mining area does not allow to exclude an anthropogenic input due to the past mining activity which preferentially affected the top-soils. The increasing values of clr.Hg seem to follow the main normal faults and associated reference structures and highlight a relatively large anomaly in this portion of the investigated territory, as already suggested by Ferrara (1999). Conversely, Sb, Co, Cr, Ni, and V clr-variables show a lower variability and their distribution patterns of clr-maps in most cases linked to the sedimentary (limestone/siliciclastic) lithology, underlining a geochemical enrichment of these metals. High relative contents of Sb in some volcanic soils are likely due to previously not recognized old mining dumps and not related to the Abbadia San Salvatore mining activity, Sb-rich minerals being mostly associated with the Siele and Morone Hg-mines. Subsequently, the two data populations (volcanic and limestone/siliciclastic) were thus considered separately and the outliers, characterizing some elements, were removed. Consequently, the geochemical baseline values of PTEs were calculated on these two datasets, only for those elements that showed concentrations higher than the Lgs.D. Since any analytical measurement is affected by an uncertainty, a concentration interval for each metal was considered more appropriate than a single value.

The geochemical and statistical approach used in this work implies that specific territories, where mining or other anthropic activities or areas affected by peculiar geological situations (e.g. presence of ore-deposits close to the surface), can be characterized by anomalous concentrations able to jeopardize the definition of soil baseline values. Consequently, the law reference values cannot be applied without any specific investigations and a detailed knowledge of the territory. Assessing the background and/or geochemical baseline values have a pivotal importance to face environmental problems that local authorities and stakeholders may have to handle and avoid unappropriated costly remediation operations and/or affect the economic growth. This is the case of the Municipality of Abbadia San Salvatore where important activities (e.g. construction of garages and the local heliport) were slowed down or even stopped as the excavated soils showed heavy metal contents (Hg and As) higher than those imposed by the Italian law but lower than the geochemical baseline values computed in this work.

Supplementary data to this article can be found online at https://doi.org/10.1016/j.gexplo.2023.107324.

CRediT authorship contribution statement

Conceptualization, FM, BN, OV and DR; methodology, FM and VR; software FM, BN and CG; formal analysis, FM and VR; investigation, FM, JC, BN, GM.; resources, OV, GM and DR; data curation, FM, OV, BN and CG; writing original draft preparation, FM, BN, JC, CG and OV. All

authors read and approved the final manuscript; funding acquisition, OV and DR. All authors have read and agreed to the published version of the manuscript.

Declaration of competing interest

The authors declare that they have no known competing financial interests or personal relationships that could have appeared to influence the work reported in this paper.

Data availability

Data will be made available on request.

Acknowledgements

Many thanks are due to Andrea Esposito and Fabrizio Piccinelli for their assistance during the field work. The work was financially supported by an agreement between the Department of Earth Sciences (Resp. Orlando Vaselli) and the Unione dei Comuni Amiata-Val d'Orcia (Resp. Daniele Rappuoli). Two reviewers and A. Buccianti are kindly thanked for their useful comments and suggestions that strongly improved an early version of the manuscript.

References

Aitchison, J., 1982. The statistical analysis of compositional data. J. R. Stat. Soc. Series B (Methodological) 44 (2), 139–160. https://doi.org/10.1111/j.2517-6161.1982.tb01195.x.

Aitchison, J., 1986. The Statistical Analysis of Compositional Data. In: Monographs on Statistics and Applied Probability. Chapman & Hall Ltd., London.

Albanese, S., De Vivo, B., Lima, A., Cicchella, D., 2007. Geochemical background and baseline values of toxic elements in stream sediments of Campania region (Italy). J. Geochem. Explor. 93, 21–34. https://doi.org/10.1016/j.gexplo.2006.07.006.

Bargagli, R., Iosco, F.P., Barghigani, C., 1987. Assessment of mercury dispersal in a abandoned mining area by soil and lichen analysis. Water, Air Soil Pollut. 36, 219–225.

Barghigani, C., Ristori, T., 1994. Mercury Levels in Agricultural Products of Mt. Amiata (Tuscany, Italy). Arch. Environ. Contamin. Toxicol. 26, 329–334.

Barghigani, C., Ristori, T., 1995. Preliminary Study on Mercury Uptake by Rosmarinus officinalis L. (Rosemary) in a Mining Area (Mt.Amiata, Italy). Bull. Environ. Contamin. Toxicol. 54, 519.

Bellani, S., Brogi, A., Lazzarotto, A., Liotta, D., Ranalli, G., 2004. Heat flow, deep temperatures and extensional structures in the Larderello Geothermal Field (Italy): constraints on geothermal fluid flow. J. Volcanol. Geotherm. Res. 132, 15–29. https://doi.org/10.1016/S0377-0273(03)00418-9.

Boente, C., Albuquerque, M.T.D., Fernández-Brañaa, A., Gerassisc, S., Sierrad, C., Gallego, J.R., 2018. Combining raw and compositional 1 data to determine the spatial patterns of potentially toxic elements in soils. Sci. Total Environ. 631–632, 1117–1126. https://doi.org/10.1016/j.scitotenv.2018.03.048.

Botticelli, M., 2019. Archaeometric Investigations on Red Pigments: The Provenance of Cinnabar and the Discrimination of Synthetic and Natural Ochres (PhD Thesis). University of Rome "La Sapienza", p. 271.

Brogi, A., Liotta, B., 2017. Le strutture tettoniche quaternarie nelle vulcaniti del Monte Amiata e dintorni. In: E.S.A-Edizioni Scientifiche e Artistiche (Ed.). Il Vulcano di Monte Amiata, Nola (NA), Italy, pp. 55–70.

Brogi, A., Liotta, D., Meccheri, M. Fabbrini, L., 2010. Transtensional shear zones controlling volcanic eruptions: the Middle Pleistocene Monte Amiata volcano (inner Northern Apennines, Italy). Terra Nova 22, 137–146. https://doi.org/10.1111/j.1365-3121.2010.00927.x.

Brogi, A., Fabbrini, L., Liotta, D., 2011. Sb–Hg ore deposit distribution controlled by brittle structures: the case of the Selvena mining district (Monte Amiata, Tuscany, Italy). Ore Geol. Rev. 41, 35–48. https://doi.org/10.1016/j.oregeorev.2011.06.004.

Buccianti, A., Pawlowsky-Glahn, V., 2005. New perspectives on water chemistry and compositional data analysis. Math. Geol. 37, 703–727. https://doi.org/10.1007/s11004-005-7376-6.

Buccianti, A., Lima, A., Albanese, S., De Vivo, B., 2018. Measuring the change under compositional data analysis (CoDA): Insight on the dynamics of geochemical systems. J. Geochem. Expl. 189, 100–108.

Cabral Pinto, M.M.S., Silva, M.M.V.G., Ferriera da Silva, E.A., Dinis, P.A., Rocha, F., 2017. Transfer processes of potentiallu toxic elements (PTE) from rocks to soils and the origin of PTE in soils: a case study on the island of Santiago (Cape Verde). J. Geochem. Expl. 183, 140–151. https://doi.org/10.1016/j.gexplo.2017.06.004.

Cave, M.R., Johnson, C.C., Ander, E.L., Palumbo-Roe, B., 2012. Methodology for the determination of normal background contaminant concentrations in English soils. In: British Geological Survey Commissioned Report, CR/12/003. Available at:. http://nora.nerc.ac.uk/19959/.

Chiarantini, L., Benvenuti, M., Beutel, M., Costagliola, P., Covelli, S., Gabbani, G., Lattanzi, P., Pandeli, E., Paolieri, M., Petranich, E., Rimondi, V., 2016. Mercury and arsenic in stream sediments and surface waters of the orcia river basin, southern Tuscany, Italy. Water Air Soil Pollut. 227 https://doi.org/10.1007/s11270-016-3110-x.

Cicchella, D., De Vivo, B., Lima, A., 2005. Background and baseline concentration values of elements harmful to human health in the volcanic soils of the metropolitan provincial area of Napoli (Italy). Geochem. Explor. Environ. Anal. 5, 29–40. https://doi.org/10.1144/1467-7873/03-042.

Cicchella, D., Ambrosino, M., Gramazio, A., Coraggio, F., Musto, M.A., Caputi, A., Avagliano, D., Albanese, S., 2022. Using multivariate compositional data analysis (CoDA) and clustering to establish geochemical backgrounds in stream sediments of an onshore oil deposits area. The Agri River basin (Italy) case study. J. Explor. Geochem. 238, 107012 https://doi.org/10.1016/j.gexplo.2022.107012.

Cipriani, C., Tanelli, G., 1983. Risorse minerarie ed industria estrattiva in Toscana. Note storiche ed economiche. Atti e Memorie Accademia di Scienze e Lettere La Colombaria, 28, pp. 241–283 (in Italian).

Condie, K.C., 1993. Chemical composition and evolution of the upper continental crust: contrasting results from surface samples and shales. Chem. Geol. 104, 1–37. https://doi.org/10.1016/0009-2541(93)90140-E.

Conticelli, S., Boari, E., Burlamacchi, L., Cifelli, F., Moscardi, F., Laurenzi, M.A., Ferrari, Pedraglio L., Francalanci, L., Benvenuti, M.G., Braschi, E., Moretti, P., 2015. Geochemistry and Sr-Nd-Pb isotopes of Monte Amiata volcano, Central Italy: evidence for magma mixing between high-K calc-alkaline and leucititic mantle-derived magmas. Ital. J. Geosci. 132 (2), 266–290 (10.3301/IJG.2015.12).

Crane, J.L., Bijak, A.L., Maier, M.A., Nord, M.A., 2021. Development of current ambient background threshold values for sediment quality parameters in US lakes on a regional and statewide basis. Sci. Total Environ. 793, 148630 https://doi.org/10.1016/j.scitotenv.2021.148630.

Daunis-I-Estadella, J., Barceló-Vidal, C., Buccianti, A., 2006. Exploratory compositional data analysis. Geol. Soc. Lond. Sp. Publ. 264, 161–174.

Dini, A., 2003. Ore deposits, industrial minerals and geothermal resources. In: Poli, G., Perugini, D., Rocchi, S., Dini, A. (Eds.), Miocene to Recent Plutonism and Volcanism in the Tuscan Magmatic Province, Per. Mineral., Spec. Is, 72, pp. 41–52.

Dini, A., 2017. Mines and minerals in the Mining district of Monte Amiata. In: E.S.A-Edizioni Scientifiche e Artistiche (Ed.), Il Vulcano di Monte Amiata. Nola (NA), Italy, pp. 343–369.

Egozcue, J.J., Pawlowsky-Glahn, V., Mateu-Figueras, G., Barceló-Vidal, C., 2003. Isometric logratio transformations for compositional data analysis. Math. Geol. 35, 270–300.

Facchinelli, A., Sacchi, E., Mallen, L., 2001. Multivariate statistical and GIS-based approach to identify heavy metal sources in soils. Environ. Pollut. 114, 313–324. https://doi.org/10.1016/S0269-7491(00)00243-8.

Fantoni, R., Lazic, V., Colao, F., Almaviva, S., Puiu, A., 2022. Caracterización del color rojo en varios frescos y pinturas romanas in situ y remotas mediante espectroscopías LIBS, LIF y Raman. Ge-Conservacion 21 (1), 257–269. https://doi.org/10.37558/gec.v21i1.1117.

Ferrara, R., 1999. Mercury Mines in Europe: Assessment of Emissions and Environmental Contamination. Mercury Contaminated Sites: Characterization, Risk Assessment and Remediation, pp. 51–72.

Ferrara, R., Mazzolai, U.B., Edner, H., Svanberg, S., Wallinder, E., 1998. Atmospheric mercury sources in the Mt. Amiata area, Italy. SciTotal Environ. 213, 12–23.

Ferrari, L., Conticelli, S., Burlamachi, L., Manetti, P., 1996. Volcanological evolution of the Monte Amiata, Southern Tuscany: new geological and petrochemical data. Acta Vulcanol. 8, 41–56.

Filzmoser, P., Hron, K., Reimann, C., 2009. Univariate statistical analysis of environmental (compositional) data: problems and possibilities. Sci. Total Environ. 407, 6100–6108.

Filzmoser, P., Hron, K., Templ, M., 2018. Applied Compositional Data Analysis: With Worked Exeples in R. Springer. https://doi.org/10.1007/978-3-319-96422-5.

Forconi, S., 2011. Il Cinabro sul Monte Amiata. Stampa 2000, 223 (In Italian).

Frattini, P., De Vivo, B., Lima, A., Cicchella, D., 2006. Background and baseline values of human health harmful elements and gamma-ray survey in the volcanic soils of Ischia island (Italy). Geochem.: Explor., Environ., Anal. 6, 325–339. ISSN: 1467-7873. https://doi.org/10.1144/1467-7873/06-105.

Galan, E., Fernandez-Caliani, J.C., Gonzalez, I., Aparicio, P., Romero, A., 2008. Influence of geological setting on geochemical baselines of trace elements in soils. Application to soils of South-West Spain. J. Geochem. Expl. 98, 89–106. https://doi.org/10.1016/j.gexplo.2008.01.001.

Gao, S., Luo, T.C., Zhang, B.R., Zhang, H.F., Han, Y.W., Zhao, Z.D., Hu, Y.K., 1998. Chemical composition of the continental crust as revealed by studies in East China. Geochim. Cosmochim. Acta 62, 1959–1975. https://doi.org/10.1016/S0016-7037(98)00121-5ISS.

Geochemical Earth Reference Model (GERM) Reservoir Database. http://earthref.org/GERMRD/reservoirs/ (Accessed on 29/04/2023).

Ghezelbash, R., Maghsoudi, A., Carranza, E.J.M., 2019. Mapping of single- and multi-element geochemical indicators based on catchment basin analysis: Application of fractal method and unsupervised clustering models. J. Geochem. Expl. 199, 90–104. https://doi.org/10.1016/j.gexplo.2019.01.017.

Ghezelbash, R., Maghsoudi, A., Carranza, E.J.M., 2020. Optimization of geochemical anomaly detection using a novel genetic K-means clustering (GKMC) algorithm. Comput. Geosci. 134, 104335.

Giaccio, L., Cicchella, D., De Vivo, B., Lombardi, G., De Rosa, M., 2012. Does heavy metals pollution affects semen quality in men? A case of study in the metropolitan area of Naples (Italy). J. Geochem. Explor. 112, 218–225. https://doi.org/10.1016/j.gexplo.2011.08.009.

Gianelli, G., Puxeddu, M., Batini, F., Bertini, G., Dini, I., Pandeli, E., Nicolich, R., 1988. Geological model of a young volcano-plutonic system: the geothermal region of Monte Amiata (Tuscany, Italy). Geothermics 17 (5–6), 719–734. https://doi.org/10.1016/0375-6505(88)90033-8.

Gilbert, R.O., 1987. Statistical Methods for Environmental Pollution Monitoring. John Wiley & Sons Ltd, New York (ISBN 0-471-28878-0).

Gozzi, C., 2020. Weathering and transport processes investigated through the statistical properties of the geochemical landscapes: the case study of the Tiber river basin (Central Italy). Plinius 46, 48–55. https://doi.org/10.19276/plinius.2020.01007.

Gozzi, C., Sauro Graziano, R., Buccianti, A., 2020. Part-whole relations: new insights about the dynamics of complex geochemical riverine systems. Minerals. 10 (6), 501. https://doi.org/10.3390/min10060501.

Gozzi, C., Dakos, V., Buccianti, A., Vaselli, O., 2021. Are geochemical regime shifts identifiable in river waters? Exploring the compositional dynamics of the Tiber River (Italy). Sci. Total Environ. 785, 147268 https://doi.org/10.1016/j.scitotenv.2021.147268.

IRSA-CNR, 1985. N°64: Metodi analitici per i fanghi. Parametri chimico-fisici. In Italian.

Johnson, C.C., Ander, E.L., Cave, M.R., Palumbo-Roe, B., 2012. Normal Background Concentrations (NBCs) of Contaminants in English Soils: Final Project Report. British Geological Survey Commissioned Report. CR/12/035, 40 pp. Available at: http://nora.nerc.ac.uk/19946/.

Kabata-Pendias, A., 2010. Trace Elements in Soils and Plants, 4th edition. CRC Press. https://doi.org/10.1201/b10158. 549 p.

Karn, R., Ojha, N., Abbas, S.M., Burg, S., 2021. A review on heavy metal contamination at mining sites and remedial techniques. OP Conf. Ser.: Earth Environ. Sci. 796, 012013. https://doi.org/10.1088/1755-1315/796/1/012013.

Kassambara, A., Mundt, F., 2019. Factoextra: extract and visualize the results of multivariate data analyses. R package version 1 (5), 337–354.

Kemp, A.I.S., Hawkesworth, C.J., 2004. Granitic perspectives on the generation and secular evolution of the continental crust. In: Holland, H.D., Turekian, K.K. (Eds.), Treatise on Geochemistry, v. 3. Elsevier, Amsterdam, pp. 349–410.

Klemm, D.D., Neumann, N., 1984. Ore-controlling factors in the Hg–Sb province of southern Tuscany, Italy. In: Wauschkuhn, A., Kluth, C., Zimmermann, R.A. (Eds.), Syngenesis and Epigenesis in the Formation of Mineral Deposits. Springer-Verlag, Heidelberg, pp. 482–503.

Kynčlová, P., Hron, K., Filzmoser, P., 2017. Correlation between compositional parts based on symmetric balances. Math. Geosci. https://doi.org/10.1007/s11004-016-9669-3.

Laurenzi, M.A., Braschi, E., Casalini, M., Conticelli, S., 2015. New 40Ar-39Ar dating and revision of the geochronology of the Monte Amiata Volcano, Central Italy. Italian J. Geosci. 134, 255–265.

Liotta, D., 1991. The Arbia-Val Marecchia line, north Apennines. Ecl. Geol. Helv 84, 413–430.

Liotta, D., 1996. Analisi del settore centro-meridionale del bacino pliocenico di Radicofani (Toscana meridionale). Boll. Soc. Geol. It. 115, 115–143 (In Italian with English abstract).

Marchand, C., Allenbach, M., Lallier-Verges, E., 2011. Relationships between heavy metals distribution and organic matter cycling in mangrove sediments (Conception Bay, New Caledonia). Geoderma 160, 444–456. https://doi.org/10.1016/j.geoderma.2010.10.015.

Marroni, M., Moratti, G., Costantini, A., Conticelli, S., Benvenuti, M.G., Pandolfi, L., Bonini, M., Cornamusini, G., Laurenzi, M.A., 2015. Geology of the Monte Amiata region, Southern Tuscany, Central Italy. Ital. J. Geosci. 134, 171–199 (doi:10.3301/IJG.2015.13).

Martini, I.P., Sagri, M., 1993. Tectono-sedimentary characteristics of Late Miocene-Quaternary extensional basins of the Nothern Apennines. Earth Sci. Rev. 34, 197–233.

Mazurek, R., Kowalska, J., Gasiorek, M., Zadrozny, P., Jozefowska, A., Zaleski, T., Kepka, W., Tymczuk, M., Orlowska, K., 2017. Assessment of heavy metals contamination in surface layers of Roztocze National Park forest soils (SE Poland) by indices of pollution. Chemosphere 168, 839–850. https://doi.org/10.1016/j.chemosphere.2016.10.126.

McKinley, J.M., Hron, K., Grunsky, E., Reimann, C., de Caritat, P., Filzmoser, P., Van den Boogaart, K.G., Tolosana-Delgado, R., 2016. The single component geochemical map: fact or fiction. J. Geochem. Explor. 162, 16–28. https://doi.org/10.1016/j.gexplo.2015.12.005.

Meloni, F., 2022. Determinazione dei valori di fondo di Cr, Co, Ni nel Bacino del Torrente Stura (Comune di Barberino di Mugello). Il Geologo 16, 27–33 (In Italian).

Meloni, F., Montegrossi, G., Lazzaroni, M., Rappuoli, D., Nisi, B., Vaselli, O., 2021. Total and leached arsenic, mercury and antimony in the mining waste dumping area of Abbadia San Salvatore (Mt. Amiata, Central Italy). Appl. Sci. 11, 7893. https://doi.org/10.3390/app11177893.

Morteani, G., Ruggieri, G., Möller, P., Preinfalk, C., 2011. Geothermal mineralized scales in the pipe system of the geothermal Piancastagnaio power plant (Mt. Amiata geothermal area): a key to understand the stibnite, cinnabarite and gold mineralization of Tuscany (central Italy). Miner. Dep. 46, 197–210.

Nordstrom, D., 2015. Baseline and premining geochemical characterization of mined sites. Appl. Geochem. 17-34, 57. https://doi.org/10.1016/j.apgeochem.2014.12.010.

Nriagu, J., Pacyna, J., 1988. Quantitative assessment of worldwide contamination of air, water and soils by trace metals. Nature 333, 134–139. https://doi.org/10.1038/333134a0.

Palarea-Albaladejo, J., Martin-Fernandez, J., 2015. Compositions: Treatment of Zeros, Left-Censored and Missing Values in Compositional Data Sets (accessed on 28/08/2023).

Pandeli, E., Bertini, G., Castelluct, P., Morelli, M., Monechi, S., 2005. The sub-Ligurian and Ligurian units of the Mt. Amiata geothermal region (south-eastern Tuscany): new stratigraphic and tectonic data and insights into their relationships with the Tuscan Nappe. Boll. Soc. Geol. It. Sp. Issue 3, 55–71.

Pandeli, E., Bertini, G., Orti, L., 2017. Inquadramento geologico regionale dell'area del Monte Amiata. In: E.S.A-Edizioni Scientifiche e Artistiche (Ed.), Il Vulcano di Monte Amiata. Nola (NA), pp. 21–54 (In Italian).

Pasquetti, F., Vaselli, O., Zanchetta, G., Nisi, B., Lezzerini, M., Bini, M., Mele, D., 2020. Sedimentological, mineralogical and geochemical features of Late Quaternary sediment profiles from the southern Tuscany Hg mercury district (Italy): evidence for the presence of pre-industrial mercury and arsenic concentrations. Water 2020 (12), 1998. https://doi.org/10.3390/w12071998.

Pawlowsky-Glahn, V., Buccianti, A., 2011. Compositional Data Analysis: Theory and Applications. John Wiley & Sons Ltd., p. 400

Pawlowsky-Glahn, V., Egozcue, J.J., 2001. Geometric approach to statistical analysis on the simplex. In: SERRA.15, pp. 384–398.

Pawlowsky-Glahn, V., Egozcue, J.J., 2020. Compositional data in geostatistics: A log-ratio based framework to analyze regionalized compositions. Math. Geosci. 52, 1067–1084. https://doi.org/10.1007/s11004-020-09873-2.

Pourret, O., Hursthouse, A., 2019. It's time to replace the term "heavy metals" with "potentially toxic elements" when reporting environmental research. Intern. J. Environ. Res. Public Health 16, 4446. https://doi.org/10.3390/ijerph16224446.

Pribil, M.J., Rimondi, V., Costagliola, P., Lattanzi, P., Rutherford, D.L., 2020. Assessing mercury distribution using isotopic fractionation of mercury processes and sources adjacent and downstream of a legacy mine district in Tuscany, Italy. Appl. Geochem. 117 https://doi.org/10.1016/j.apgeochem.2020.104600.

Principe, C., Vezzoli, L., La Felice, S., 2018. Geology of Monte Amiata volcano (Southern Tuscany). Alp. Medit. Quat. 31, 235–238.

Protano, G., Nannoni, F., 2018. Influence of ore processing activity on Hg, As and Sb contamination and fractionation in soils in a former mining site of Monte Amiata ore district (Italy). Chemosphere. 199, 320–330. https://doi.org/10.1016/j.chemosphere.2018.02.051.

Qingjie, G., Jun, D., 2008. Calculating pollution indices by heavy metals in ecological geochemistry assessment and a case study in parks of Beijing. J. Chin. Univ. Geosci. 19, 230–241. https://doi.org/10.1016/S1002-0705(08)60042-4.

R Core Team, R., 2021. A Language and Environment for Statistical Computing. R Foundation for Statistical Computing, Vienna, Austria. Available online: https://www.R-project.org/ (accessed on 15/01/2022).

Reiman, C., de Caritat, P., 2017. Establishing geochemical background variation and threshold values for 59 elements in Australian surface soil. Sci. Total Environ. 578, 633–648. https://doi.org/10.1016/j.scitotenv.2016.11.010.

Reimann, C., de Caritat, P., 1998. Chemical Elements in the Environment - Factsheets for the Geochemist and Environmental Scientist. Springer-Verlag, Berlin, Germany, p. 388.

Reimann, C., de Caritat, P., 2005. Distinguishing between natural and anthropogenic sources for elements in the environment: regional geochemical surveys versus enrichment factors. Sci. Total Environ. 337 (2005), 91–107. https://doi.org/10.1016/j.scitotenv.2004.06.011.

Reimann, C., Filzmoser, P., Garrett, R.G., Dutter, R., 2008. Statistical Data Analysis Explained: Applied Environmental Statistics With R. John Wiley & Sons Ltd.

Reimann, C., Filzmoser, P., Fabian, K., Hron, K., Birke, M., Demetriades, A., Dinelli, E., Ladenberger, A., GEMAS Project Team, 2012. The concept of compositional data analysis in practice - total major element concentrations in agricultural and grazing land soils of Europe. Sci. Total Environ. 426, 196–210.

Reimann, C., Filzmoser, P., Hron, K., Kynclovà, P., Garrett, R.G., 2017. A new method for correlation analysis of compositional (environmental) data-a worked example. Sci. Total Environ. 607-608, 956–971. https://doi.org/10.1016/j.scitotenv.2017.06.063.

Rimondi, V., Gray, J.E., Costagliola, P., Vaselli, O., Lattanzi, P., 2012. Concentration, distribution, and translocation of mercury and methylmercury in mine-waste, sediment, soil, water, and fish collected near the Abbadia San Salvatore mercury mine, Monte Amiata district, Italy. Sci. Total Environ. 414, 318–327. https://doi.org/10.1016/j.scitotenv.2011.10.065.

Rimondi, V., Bardelli, F., Benvenuti, M., Costagliola, P., Gray, J.E., Lattanzi, P., 2014. Mercury speciation in the Mt. Amiata mining district (Italy): interplay between urban activities and mercury contamination. Chem. Geol. 221–226. https://doi.org/10.1016/j.chemgeo.2014.04.023.

Rimondi, V., Chiaranti, L., Lattanzi, P., Benvenuti, M., Beutel, M., Colica, A., Costagliola, P., Di Bendetto, F., Gabbani, G., Gray, J.E., Pandeli, E., Pattelli, G., Paolieri, M., Ruggieri, G., 2015. Metallogeny, explotation and environmental impact of the Mt. Amiata mercury ore district (Southern Tuscany, Italy). Ital. J. Geosci. 134, 323–336 (doi:10.3301/IJG.2015.02).

Risch, R.M., DeWild, J.F., Krabbenhoft, D.P., Kolka, R.K., Zhang, L., 2012. Litterfall mercury dry deposition in the eastern USA. Environ.Pollut. 161, 284–290. https://doi.org/10.1016/j.envpol.2011.06.005.

Sahoo, P.K., Dall'Agnol, R., Salomao, G.N., Da Silva Ferreira Junior, J., Silva, M.S., Martins, P.W., Filho, S., Da Costa, L.M., Angelica, R.S., Medeiros Filho, C.A., da Costa, M.F., Guimaraes Guilherme, L.R., Siqueira, J.O., 2020. Regional-scale mapping for determining geochemical background values in soils of the Itacaiunas River Basin, Brazil: the use of compositional data analysis (CoDA). Geoderma 376, 114504. https://doi.org/10.1016/j.geoderma.2020.114504.

Salminen, R., Gregorauskiene, V., 2000. Consideration regarding the definition of a geochemical baseline of elements in the surficial materials in areas differing in basic geology. J. Appl. Geochem. 15, 647–653.

Salminen, R., Tarvainen, T., 1997. The problem of defining geochemical baselines. A case study of selected elements and geological materials in Finland. J. Geochem. Explor. 60, 91–98.

Salminen, R.(Chef. Edit), Batista, M.J., Bidovec, M., Demetriades, A., De Vivo, B., De Vos, W., Duris, M., Gilucis, A., Gregorauskiene, V., Halamic, J., Heitzmann, P., Lima, A., Jordan, G., Klaver, G., Klein, P., Lis, J., Locutura, J., Marsina, K., Mazreku, A., O'Connor, P.J., Olsson, S.Å., Ottesen, R.T., Petersell, V., Plant, J.A., Reeder, S., Salpeteur, I., Sandström, H., Siewers, U., Steenfelt, A., Tarvainen, T., 2005. Geochemical Atlas of Europe. Part 1 - Background Information, Methodology and Maps.

Santos-Francés, F., Martinez-Grana, A.A., Alonso-Rojo, P., Garcia-Sanchez, A., 2017. Geochemical background and baseline values determination and spatial distribution of heavy melta polution in soils of the Andes mountain range (Cajamarca-Huancavelica, Peru). Int. J. Envron. Res. Public Health 14, 859. https://doi.org/10.3390/ijerph14080859.

Singh, A., Maichle, R., 2015. ProUCL Version 5.1 user guide. U.S. Environmental Protection Agency, Washington, DC. EPA/600/R-07/041. https://www.epa.gov/sites/production/files/2016-05/documents/proucl_5.1_user-guide.pdf.

SNPA, 2017. Linea guida per la determinazione dei valori di fondo per i suoli e per le acque sotterranee (ISBN 978-88-448-0880-8).

Sodo, A., Artioli, D., Botti, A., De Palma, G., Giovagnoli, A., Mariottini, M., Paradisi, A., Polidoro, C., Ricci, M.A., 2008. The colours of Etruscan painting: a study on the Tomba dell'Orco in the necropolis of Tarquinia. J. Raman Spectrosc. 39, 1035–1041. https://doi.org/10.1002/jrs.1982.

Staudigel, H., Albarede, F., Shaw, H., McDonough, B., White, W., 1996. The Geochemical Earth Reference Model (GERM). American Geophysical Union Fall Meeting, San Francisco (USA), p. 13. December 1996.

Tanelli, G., 1983. Mineralizzazioni metallifere e minerogenesi della Toscana. Mem. Soc. Geol. Ital. 25, 91–109 (in Italian).

Tarvainen, T., Kallio, E., 2002. Baselines of certain bioavailable and total heavy metal concentrations in Finland. J. Appl. Geochem. 17, 975–980.

Templ, M., Hron, K., Filzmoser, P., 2011. Robcompositions: an R-package for robust statistical analysis of compositional data. In: Compositional Data Analysis: Theory and Applications. John Wiley & Sons Ltd, pp. 341–355.

Turkey, J.W., 1977. Exploratory data analysis. J. Exp. Psychol. 87 2, 131–160.

USEPA, 2022. ProUCL: Statistical Software for Environmental Applications for Data Sets With and Without Nondetect Observations. Version 5.2. https://www.epa.gov/land-research/proucl-software.

Vaselli, O., Higueras, P., Nisi, B., Esbrì, J.M., Cabassi, J., Martìnez-Coronado, A., Tassi, F., Rappuoli, D., 2013. Distribution of gaseous Hgin the Mercury mining district of Mt. Amiata (Central Italy): a geochemical survey prior the reclamation project. Environ. Res. 125, 179–187. https://doi.org/10.1016/j.envres.2012.12.010.

Vaselli, O., Nisi, B., Rappuoli, D., Cabassi, J., Tassi, F., 2017. Gaseous elemental mercury and total and leached mercury in buildingmaterials from the former Hg-mining area of Abbadia San Salvatore (Central Italy). Int. J. Environ. Res. Public Health 14. https://doi.org/10.3390/ijerph14040425.

Vaselli, O., Rappuoli, D., Bianchi, F., Nisi, B., Niccolini, M., Esposito, A., Cabassi, J., Giannini, L., Tassi, F., 2019. One hundred years of mercury exploitation at the mining area of Abbadia San Salvatore (Mt. Amiata, Central Italy): a methodological approach fro a complex reclamation activity before the establishment of a new mining park. In: El patrimonio geològico y minero. Identidad y motor de desarrollo. Publicaciones del Instituto Geològico y minero de España Serie: Cuadernos del Museo Geominero, n. 29. Proceed. XVII Congreso Internacional sobre Patrimonio Geológico y Minero, pp. 1109–1126. ISBN: 978-84-9138-081-8, 21-24 September 2017, Almaden (Spain).

Vezzoli, L., Principe, C., 2023. Building a silicic effusive volcano: geology, structure, and tectonics of Monte Amiata (Middle Pleistocene, Italy). J. Volcanol. Geotherm. Res. 434, 107743 https://doi.org/10.1016/j.jvolgeores.2022.107743.